confirmed by Western blotting using anti FLAG-M2 (Sigma) and anti-HepC-NS5b (Santa Cruz Biotechnology) antibodies.

For RCYM1 cells, after preparing the cytoplasmic extract, immunoprecipitation was carried out using the anti-HepC-NS5b (Santa Cruz Biotechnology) antibody.

The eluates from the immunoprecipitation were treated with proteinase K to release the NS5B-bound RNA molecules. RNA was isolated using TRIzol reagent (Invitrogen) as instructed by the manufacturer, followed by DNase treatment to completely remove the cellular genomic DNA. For detecting mRNA molecules bound to NS5B, RT-PCR was performed using gene-specific primer pairs for GAL-1 (5′-GGACCGAGCAGCGGGAGG-3′ and 5′-CAGGGGAGCAGAGG-CAGC-3′; a 250-bp product; annealing temperature: 61 °C), RPS4X (5′-CGACTTTCCAACATTTTT-3′ and 5′-TGCTATTAATCCTGCCAC-3′; a 200-bp product; annealing temperature: 52 °C) or FOXK1 (5′-CGCG-GCGGCCTGTGGGCA-3′ and 5′-TGCGTTTCTGTCTGTCCT-3′; a 300-bp product; annealing temperature: 61 °C), respectively. The primer pairs for GAL-1 and RPS4X were designed to amplify the full length 3′-UTRs plus the 3′-end coding sequences, respectively, while the one for FOXK1 was designed to amplify the segment within the 3′-UTR of FOXK1. The PCR products were electrophoresed on 5% polyacrylamide gels and stained with ethidium bromide.

Acknowledgments

We would like to thank Prof. H. Aburatani at the Genome Science Division, Research Center for Advanced Science and Technology, The University of Tokyo for helpful discussion. We also thank S. Kawanabe for technical support.

This work was supported by New Energy and Industrial Technology Development Organization (NEDO) and carried out in cooperation with Japan Biochemistry Association (JBA).

References

Ago, H., Adachi, T., Yoshida, A., Yamamoto, M., Habuka, N., Yatsunami, K., Miyano, M., 1999. Crystal structure of the RNA-dependent RNA polymerase of hepatitis C virus. Structure 7, 1417–1426.

Antic, D., Lu, N., Keene, J.D., 1999. ELAV tumor antigen, Hel-N1, increases translation of neurofilament M mRNA and induces formation of neurites in human teratocarcinoma cells. Genes Dev. 13, 449–461.

Behrens, S.E., Tomei, L., De Francesco, R., 1996. Identification and properties of the RNA-dependent RNA polymerase of hepatitis C virus. EMBO J 15, 12–22.

Biroccio, A., Hamm, J., Incitti, I., De Francesco, R., Tomei, L., 2002. Selection of RNA aptamers that are specific and high-affinity ligands of the hepatitis C virus RNA-dependent RNA polymerase. J. Virol. 76, 3688–3696.

Blackham, S., Baillie, A., Al-Hababi, F., Remlinger, K., You, S., Hamatake, R., McGarvey, M.J., 2010. Gene expression profiling indicates the roles of host oxidative stress, apoptosis, lipid metabolism, and intracellular transport genes in the replication of hepatitis C virus. J. Virol. 84, 5404–5414.

Bressanelli, S., Tomei, L., Roussel, A., Incitti, I., Vitale, R.L., Mathieu, M., De Francesco, R., Rey, F.A., 1999. Crystal structure of the RNA-dependent RNA polymerase of hepatitis C virus. Proc. Natl. Acad. Sci. U.S.A. 96, 13034–13039.

Camby, I., Le Mercier, M., Lefranc, F., Kiss, R., 2006. Galectin-1: a small protein with major functions. Glycobiology 16, 137R–157R.

Cheng, J.C., Chang, M.F., Chang, S.C., 1999. Specific interaction between the hepatitis C virus NS5B RNA polymerase and the 3′ end of the viral RNA. J. Virol. 73, 7044–7049.

Choo, Q.L., Kuo, G., Weiner, A.J., Overby, L.R., Bradley, D.W., Houghton, M., 1989. Isolation of a cDNA clone derived from a blood-borne non-A, non-B viral hepatitis genome. Science 244, 359–362.

De Francesco, R., 1999. Molecular virology of the hepatitis C virus. J. Hepatol. 31 (Suppl. 1), 47–53.

Dingwall, C., Ernberg, I., Gait, M.J., Green, S.M., Heaphy, S., Karn, J., Lowe, A.D., Singh, M., Skinner, M.A., Valerio, R., 1989. Human immunodeficiency virus 1 tat protein binds trans-activation-responsive region (TAR) RNA in vitro. Proc. Natl. Acad. Sci. U.S.A. 86, 6925–6929.

Eckart, M.R., Selby, M., Masiarz, F., Lee, C., Berger, K., Crawford, K., Kuo, C., Kuo, G., Houghton, M., Choo, Q.L., 1993. The hepatitis C virus encodes a serine protease involved in processing of the putative nonstructural proteins from the viral polyprotein precursor. Biochem. Biophys. Res. Commun. 192, 399–406.

Eisenberg, E., Levanon, E.Y., 2003. Human housekeeping genes are compact. Trends Genet. 19, 362–365.

Friebe, P., Boudet, J., Simorre, J.P., Bartenschlager, R., 2005. Kissing-loop interaction in the 3′ end of the hepatitis C virus genome essential for RNA replication. J. Virol. 79, 380–392.

Gao, F.B., Carson, C.C., Levine, T., Keene, J.D., 1994. Selection of a subset of mRNAs from combinatorial 3′ untranslated region libraries using neuronal RNA-binding protein Hel-N1. Proc. Natl. Acad. Sci. U.S.A. 91, 11207–11211.

Garin, M.I., Chu, C.C., Golshayan, D., Cernuda-Morollon, E., Wait, R., Lechler, R.I., 2007. Galectin-1: a key effector of regulation mediated by CD4+CD25+ T cells. Blood 109, 2058–2065.

Grakoui, A., McCourt, D.W., Wychowski, C., Feinstone, S.M., Rice, C.M., 1993. A second hepatitis C virus-encoded proteinase. Proc. Natl. Acad. Sci. U.S.A. 90, 10583–10587.

Grillo, G., Turi, A., Licciulli, F., Mignone, F., Liuni, S., Banfi, S., Gennarino, V.A., Horner, D.S., Pavesi, G., Picardi, E., Pesole, G., 2010. UTRdb and UTRsite (RELEASE 2010): a collection of sequences and regulatory motifs of the untranslated regions of eukaryotic mRNAs. Nucleic Acids Res. 38, D75–80.

Guo, J., Yan, R., Xu, G.D., Zheng, C.Y., 2012. HCV NS5A and NS5B enhance expression of human ceramide glucosyltransferase gene. Virol. Sin. 27, 38–47.

Imai, T., Tokunaga, A., Yoshida, T., Hashimoto, M., Mikoshiba, K., Weinmaster, G., Nakafuku, M., Okano, H., 2001. The neural RNA-binding protein Musashi1 translationally regulates mammalian numb gene expression by interacting with its mRNA. Mol. Cell. Biol. 21, 3888–3900.

Kanamori, H., Yuhashi, K., Uchiyama, Y., Kodama, T., Ohnishi, S., 2009. In vitro selection of RNA aptamers that bind the RNA-dependent RNA polymerase of hepatitis C virus: a possible role of GC-rich RNA motifs in NS5B binding. Virology 388, 91–102.

Kanamori, H., Yuhashi, K., Ohnishi, S., Koike, K., Kodama, T., 2010. RNA-dependent RNA polymerase of hepatitis C virus binds to its coding region RNA stem-loop structure, 5BSL3.2, and its negative strand. J. Gen. Virol. 91, 1207–1212.

Kao, C.C., Yang, X., Kline, A., Wang, Q.M., Barket, D., Heinz, B.A., 2000. Template requirements for RNA synthesis by a recombinant hepatitis C virus RNA-dependent RNA polymerase. J. Virol. 74, 11121–11128.

Kato, N., Hijikata, M., Ootsuyama, Y., Nakagawa, M., Ohkoshi, S., Sugimura, T., Shimotohno, K., 1990. Molecular cloning of the human hepatitis C virus genome from Japanese patients with non-A, non-B hepatitis. Proc. Natl. Acad. Sci. U.S.A. 87, 9524–9528.

Kim, M., Kim, H., Cho, S.P., Min, M.K., 2002. Template requirements for de novo RNA synthesis by hepatitis C virus nonstructural protein 5B polymerase on the viral X RNA. J. Virol. 76, 6944–6956.

Kim, Y.G., Yoo, J.S., Kim, J.H., Kim, C.M., Oh, J.W., 2007. Biochemical characterization of a recombinant Japanese encephalitis virus RNA-dependent RNA polymerase. BMC Mol. Biol. 8, 59.

Koeller, D.M., Casey, J.L., Hentze, M.W., Gerhardt, E.M., Chan, L.N., Klausner, R.D., Harford, J.B., 1989. A cytosolic protein binds to structural elements within the iron regulatory region of the transferrin receptor mRNA. Proc. Natl. Acad. Sci. U. S.A. 86, 3574–3578.

Kolykhalov, A.A., Feinstone, S.M., Rice, C.M., 1996. Identification of a highly conserved sequence element at the 3′ terminus of hepatitis C virus genome RNA. J. Virol. 70, 3363–3371.

Lee, H., Shin, H., Wimmer, E., Paul, A.V., 2004. cis-acting RNA signals in the NS5B C-terminal coding sequence of the hepatitis C virus genome. J. Virol. 78, 10865–10877.

Lee, Y.J., Glaunsinger, B.A., 2009. Aberrant herpesvirus-induced polyadenylation correlates with cellular messenger RNA destruction. PLoS Biol 7, e1000107.

Lesburg, C.A., Cable, M.B., Ferrari, E., Hong, Z., Mannarino, A.F., Weber, P.C., 1999. Crystal structure of the RNA-dependent RNA polymerase from hepatitis C virus reveals a fully encircled active site. Nat. Struct. Biol. 6, 937–943.

Levine, T.D., Gao, F., King, P.H., Andrews, L.G., Keene, J.D., 1993. Hel-N1: an autoimmune RNA-binding protein with specificity for 3′ uridylate-rich untranslated regions of growth factor mRNAs. Mol. Cell. Biol. 13, 3494–3504.

Lin, C., Lindenbach, B.D., Pragai, B.M., McCourt, D.W., Rice, C.M., 1994. Processing in the hepatitis C virus E2-NS2 region: identification of p7 and two distinct E2-specific products with different C termini. J. Virol. 68, 5063–5073.

Liu, F.T., Rabinovich, G.A., 2005. Galectins as modulators of tumour progression. Nat. Rev. Cancer 5, 29–41.

Lohmann, V., Korner, F., Herian, U., Bartenschlager, R., 1997. Biochemical properties of hepatitis C virus NS5B RNA-dependent RNA polymerase and identification of amino acid sequence motifs essential for enzymatic activity. J. Virol. 71, 8416–8428.

Luo, G., Hamatake, R.K., Mathis, D.M., Racela, J., Rigat, K.L., Lemm, J., Colonno, R.J., 2000. De novo initiation of RNA synthesis by the RNA-dependent RNA polymerase (NS5B) of hepatitis C virus. J. Virol. 74, 851–863.

Matarrese, P., Tinari, A., Mormone, E., Bianco, G.A., Toscano, M.A., Ascione, B., Rabinovich, G.A., Malorni, W., 2005. Galectin-1 sensitizes resting human T lymphocytes to Fas (CD95)-mediated cell death via mitochondrial hyperpolarization, budding, and fission. J. Biol. Chem. 280, 6969–6985.

McCarthy, J.E., Kollmus, H., 1995. Cytoplasmic mRNA-protein interactions in eukaryotic gene expression. Trends Biochem. Sci. 20, 191–197.

Munishkin, A.V., Voronin, L.A., Ugarov, V.I., Bondareva, L.A., Chetverina, H.V., Chetverin, A.B., 1991. Efficient templates for Q beta replicase are formed by recombination from heterologous sequences. J. Mol. Biol. 221, 463–472.

Murakami, K., Ishii, K., Ishihara, Y., Yoshizaki, S., Tanaka, K., Gotoh, Y., Aizaki, H., Kohara, M., Yoshioka, H., Mori, Y., Manabe, N., Shoji, I., Sata, T., Bartenschlager, R., Matsuura, Y., Miyamura, T., Suzuki, T., 2006. Production of infectious hepatitis C virus particles in three-dimensional cultures of the cell line carrying the genome-length dicistronic viral RNA of genotype 1b. Virology 351, 381–392.

Nomaguchi, M., Teramoto, T., Yu, L., Markoff, L., Padmanabhan, R., 2004. Requirements for West Nile virus (−)- and (+)-strand subgenomic RNA synthesis in vitro by the viral RNA-dependent RNA polymerase expressed in *Escherichia coli*. J. Biol. Chem. 279, 12141–12151.

Oh, J.W., Sheu, G.T., Lai, M.M., 2000. Template requirement and initiation site selection by hepatitis C virus polymerase on a minimal viral RNA template. J. Biol. Chem. 275, 17710–17717.

Parrish, S., Resch, W., Moss, B., 2007. Vaccinia virus D10 protein has mRNA decapping activity, providing a mechanism for control of host and viral gene expression. Proc. Natl. Acad. Sci. U.S.A. 104, 2139–2144.

Perillo, N.L., Pace, K.E., Seilhamer, J.J., Baum, L.G., 1995. Apoptosis of T cells mediated by galectin-1. Nature 378, 736–739.

Poenisch, M., Bartenschlager, R., 2010. New insights into structure and replication of the hepatitis C virus and clinical implications. Semin. Liver Dis. 30, 333–347.

Rabinovich, G.A., 2005. Galectin-1 as a potential cancer target. Br. J. Cancer 92, 1188–1192.

Ranjith-Kumar, C.T., Wen, Y., Baxter, N., Bhardwaj, K., Cheng Kao, C., 2011. A cell-based assay for RNA synthesis by the HCV polymerase reveals new insights on mechanism of polymerase inhibitors and modulation by NS5A. PloS One 6, e22575.

Romero-Lopez, C., Berzal-Herranz, A., 2009. A long-range RNA-RNA interaction between the 5′ and 3′ ends of the HCV genome. RNA 15, 1740–1752.

Ross, J., 1995. mRNA stability in mammalian cells. Microbiol. Rev. 59, 423–450.

Salatino, M., Croci, D.O., Bianco, G.A., Ilarregui, J.M., Toscano, M.A., Rabinovich, G.A., 2008. Galectin-1 as a potential therapeutic target in autoimmune disorders and cancer. Expert Opin. Biol. Ther. 8, 45–57.

Santucci, L., Fiorucci, S., Cammilleri, F., Servillo, G., Federici, B., Morelli, A., 2000. Galectin-1 exerts immunomodulatory and protective effects on concanavalin A-induced hepatitis in mice. Hepatology 31, 399–406.

Spano, D., Russo, R., Di Maso, V., Rosso, N., Terracciano, L.M., Roncalli, M., Tornillo, L., Capasso, M., Tiribelli, C., Iolascon, A., 2010. Galectin-1 and its involvement in hepatocellular carcinoma aggressiveness. Mol. Med. 16, 102–115.

Takamizawa, A., Mori, C., Fuke, I., Manabe, S., Murakami, S., Fujita, J., Onishi, E., Andoh, T., Yoshida, I., Okayama, H., 1991. Structure and organization of the hepatitis C virus genome isolated from human carriers. J. Virol. 65, 1105–1113.

Tan, B.H., Fu, J., Sugrue, R.J., Yap, E.H., Chan, Y.C., Tan, Y.H., 1996. Recombinant dengue type 1 virus NS5 protein expressed in *Escherichia coli* exhibits RNA-dependent RNA polymerase activity. Virology 216, 317–325.

Tanaka, T., Kato, N., Cho, M.J., Shimotohno, K., 1995. A novel sequence found at the 3′ terminus of hepatitis C virus genome. Biochem. Biophys. Res. Commun. 215, 744749.

Uchiyama, Y., Huang, Y., Kanamori, H., Uchida, M., Doi, T., Takamizawa, A., Hamakubo, T., Kodama, T., 2002. Measurement of HCV RdRp activity with C-terminal 21 aa truncated NS5b protein: optimization of assay conditions. Hepatol. Res. 23, 90–97.

Vo, N.V., Oh, J.W., Lai, M.M., 2003. Identification of RNA ligands that bind hepatitis C virus polymerase selectively and inhibit its RNA synthesis from the natural viral RNA templates. Virology 307, 301–316.

Warner, J.R., Knopf, P.M., Rich, A., 1963. A multiple ribosomal structure in protein synthesis. Proc. Natl. Acad. Sci. U.S.A. 49, 122–129.

Yamada, N., Tanihara, K., Takada, A., Yorihuzi, T., Tsutsumi, M., Shimomura, H., Tsuji, T., Date, T., 1996. Genetic organization and diversity of the 3′ noncoding region of the hepatitis C virus genome. Virology 223, 255–261.

Zuker, M., 2003. Mfold web server for nucleic acid folding and hybridization prediction. Nucleic Acids Res. 31, 3406–3415.

J Gastroenterol
DOI 10.1007/s00535-014-1018-z

The Japanese Society of Gastroenterology

ORIGINAL ARTICLE—LIVER, PANCREAS, AND BILIARY TRACT

Effect of *PNPLA3* rs738409 variant (I148 M) on hepatic steatosis, necroinflammation, and fibrosis in Japanese patients with chronic hepatitis C

Kohichiroh Yasui · Takahisa Kawaguchi · Toshihide Shima · Hironori Mitsuyoshi · Kojiro Seki · Rei Sendo · Masayuki Mizuno · Yoshito Itoh · Fumihiko Matsuda · Takeshi Okanoue

Received: 27 August 2014 / Accepted: 9 November 2014

Abstract
Background Host genetic factors have been suspected to influence histological liver damage in chronic liver disease. The nonsynonymous single-nucleotide polymorphism rs738409 C > G in the patatin-like phospholipase domain-containing 3 gene (*PNPLA3*, also known as adiponutrin), encoding the I148 M protein variant, has been identified as a novel genetic marker for hepatic steatosis and fibrosis in nonalcoholic fatty liver disease and alcoholic liver disease. We aimed to determine whether the *PNPLA3* rs738409 variant was associated with hepatic steatosis, necroinflammation, and fibrosis in Japanese patients with chronic hepatitis C.
Methods In a cross-sectional study in Japan, we analyzed 276 patients with chronic hepatitis C who underwent liver biopsy. Genotyping for rs738409 was performed using the TaqMan genotyping assay.
Results The frequencies of the rs738409 CC, CG, and GG genotypes were 32.6, 46.4, and 21.0 %, respectively. Multivariate analysis revealed that the GG genotype was independently associated with the presence of steatosis [odds ratio (OR) 2.58, 95 % confidence interval (CI) 1.37–4.84, $p = 0.003$], severe necroinflammatory activity (OR 2.16, 95 % CI 1.12–4.16, $p = 0.02$), and advanced fibrosis (OR 2.10, 95 % CI 1.07–4.11, $p = 0.03$), after adjustment for age, sex, body mass index, and diabetes.
Conclusions The *PNPLA3* rs738409 variant influences histological liver damage in Japanese patients with chronic hepatitis C. The G allele homozygotes are at higher risk for hepatic steatosis, severe necroinflammation, and advanced fibrosis.

Keywords *PNPLA3* · Single-nucleotide polymorphism · Hepatitis C · Steatosis · Fibrosis

Introduction

Chronic hepatitis C (CHC) is a leading cause of liver cirrhosis and hepatocellular carcinoma in many countries. Hepatic steatosis occurs in more than half of patients infected with hepatitis C virus (HCV) and appears to be associated with a more rapid progression of liver fibrosis and a lower response to interferon-α-based therapy [1–3]. Both viral and host factors, including HCV genotype 3, older age, higher body mass index (BMI), diabetes, and alcohol consumption, are thought to contribute to HCV-related steatosis, [2, 4, 5]. HCV genotype 3, which is directly responsible for steatosis, is far less frequent in Japan than in Europe or the United States.

The rate of progression of liver fibrosis varies among patients with CHC. Known risk factors for fibrosis progression include older age, male sex, higher BMI, steatosis, insulin resistance, alcohol consumption, and co-infection with human immunodeficiency virus. However, these factors remain poor predictors of fibrosis progression [6, 7].

Host genetic factors have been suspected to influence histological liver damage in chronic liver disease. The

K. Yasui · H. Mitsuyoshi · Y. Itoh
Department of Molecular Gastroenterology and Hepatology, Graduate School of Medical Science, Kyoto Prefectural University of Medicine, Kyoto, Japan

T. Kawaguchi · F. Matsuda
Center for Genomic Medicine, Kyoto University Graduate School of Medicine, Kyoto, Japan

T. Shima · K. Seki · R. Sendo · M. Mizuno · T. Okanoue (✉)
Center of Gastroenterology and Hepatology, Saiseikai Suita Hospital, 1-2 Kawazono-cho, Suita 564-0013, Japan
e-mail: okanoue@suita.saiseikai.or.jp

Published online: 26 November 2014

nonsynonymous single-nucleotide polymorphism rs738409 C > G in the patatin-like phospholipase domain-containing 3 gene (*PNPLA3*, also known as adiponutrin), encoding an isoleucine to methionine substitution at residue 148 (I148 M), was initially associated with hepatic fat content in the first genome-wide association study (GWAS) on nonalcoholic fatty liver disease (NAFLD) [8]. The GWAS showed that the G allele of rs738409 influenced hepatic fat content independently of BMI, insulin resistance, and dyslipidemia. There has been growing evidence that the rs738409 variant (I148 M) is associated with steatosis, steatohepatitis, fibrosis, and cirrhosis both in NAFLD [9–11] and alcoholic liver disease [12–14]. Our GWAS of Japanese patients with NAFLD revealed that the G allele of rs738409 is associated only with typical nonalcoholic steatohepatitis with fibrosis (i.e., type 4 in Matteoni's classification [15]—not with simple steatosis or with steatosis with lobular inflammation or ballooning degeneration (i.e., types 1–3) [16].

Recent studies have suggested that the rs738409 variant is associated with hepatic steatosis and fibrosis in European patients with CHC [17, 18]. The influence of the rs738409 variant may be different in different populations. For example, the effect of the rs738409 variant on hepatic fat content is more evident among Hispanic-Americans, in whom the G allele of rs738409 is more frequent, when compared with European-Americans and African-Americans [8]. In the present cross-sectional study, we aimed to examine whether the *PNPLA3* rs738409 C > G variant (I148 M) is associated with hepatic steatosis, necroinflammation, and fibrosis in Japanese patients with CHC.

Methods

Patients

This study included a total of 276 Japanese patients with CHC who underwent liver biopsy between 2009 and 2012 at the Saiseikai Suita Hospital and the Hospital of Kyoto Prefectural University of Medicine. Inclusion criteria were as follows: patients older than 18 years, positive for anti-HCV, and positive for serum HCV-RNA. Exclusion criteria included consumption of more than 20 g of alcohol per day, positivity for hepatitis B virus surface antigen, the presence of other types of liver diseases (e.g., primary biliary cirrhosis, autoimmune hepatitis, Wilson's disease, or hemochromatosis), previous treatment with drugs known to produce hepatic steatosis, and a history of gastrointestinal bypass surgery. None of the patients had received any antiviral therapy before the liver biopsy although many of the patients had received ursodeoxycholic acid and herbal medicines.

The Ethics Committee of the Saiseikai Suita Hospital and the Kyoto Prefectural University of Medicine approved this study. Informed consent was obtained from each patient in accordance with the Declaration of Helsinki.

Laboratory tests

Clinical and laboratory data were collected at the time of liver biopsy. Body mass index (BMI) was calculated using the following formula: weight in kilograms/(height in meters)^2. Diabetes was defined as a fasting plasma glucose concentration of $\geq$126 mg/dl or a 2-h plasma glucose concentration of $\geq$200 mg/dl during an oral glucose (75 g) tolerance test or by the use of insulin or oral hypoglycemic agents to control blood glucose [19].

Venous blood samples were taken in the morning of the day of liver biopsy after a 12-h overnight fast. The laboratory evaluation included a blood cell count and measurement of serum aspartate aminotransferase (AST), alanine aminotransferase (ALT), γ-glutamyl transpeptidase (γ-GTP), and albumin. These parameters were measured using standard clinical chemistry techniques. HCV genotype was determined according to the classification of Simmonds et al. [20], and the serum HCV-RNA level was quantified as described previously [5].

Histopathological examination

Histopathological examination of the liver was performed as described previously [5]. The degrees of inflammation and fibrosis were evaluated according to the METAVIR scoring system [21].

Genotyping

DNA was extracted from peripheral blood mononuclear cells using the Gentra Puregene kit (Qiagen, Germantown, MD, USA) according to the manufacturer's protocol. DNA concentration and purity were measured with a NanoDrop 1000 spectrophotometer (Thermo Scientific, Waltham, MA, USA). Genotyping for rs738409 was performed using the TaqMan SNP genotyping assay (Applied Biosystems, Foster City, CA, USA).

Statistical analysis

Statistical analyses were performed using SPSS Statistics 22 (IBM, Chicago, IL, USA) or R (http://www.r-project.org/). To evaluate the association between the rs738409 genotypes and clinical parameters, we used the Jonckheere–Terpstra trend test (for continuous variables) and the Cochran–Armitage trend test (for categorical variables). Logistic regression analysis was used for multivariate

Table 1 Patient characteristics

Characteristic	Total	*PNPLA3* rs738409			P^a
		CC	CG	GG	
n	276 (100)	90 (32.6)	128 (46.4)	58 (21.0)	
Age (years)	58.2 ± 13.0	59.5 ± 11.9	57.7 ± 13.3	57.1 ± 13.7	0.29
Male sex	112 (40.6)	36 (40.0)	50 (39.1)	26 (44.8)	0.61
BMI (kg/m^2)	23.0 ± 3.4	23.0 ± 3.7	22.9 ± 3.4	23.1 ± 2.8	0.49
Diabetes	13 (4.7)	4 (4.4)	6 (4.7)	3 (5.2)	0.84
Platelet count ($\times 10^4/\mu l$)	16.0 ± 5.8	15.5 ± 5.1	16.4 ± 6.3	16.0 ± 5.7	0.52
AST (IU/l)	58.7 ± 43.6	61.7 ± 53.7	58.2 ± 38.7	55.0 ± 36.4	0.95
ALT (IU/l)	67.4 ± 58.0	69.2 ± 61.0	68.4 ± 60.1	62.3 ± 48.4	0.92
γ-GTP (IU/l)	59.8 ± 79.4	62.8 ± 94.3	57.5 ± 69.9	60.3 ± 74.8	0.53
Albumin (g/dl)	4.0 ± 0.5	4.0 ± 0.5	4.0 ± 0.5	4.1 ± 0.4	0.27
HCV genotype					0.09
1	198 (71.7)	55 (61.1)	102 (79.7)	41 (70.7)	
2	76 (27.5)	33 (36.7)	26 (20.3)	17 (29.3)	
ND	2 (0.8)	2 (2.2)	0 (0)	0 (0)	
HCV RNA level (logIU/ml)	6.0 ± 1.1	6.0 ± 1.1	6.1 ± 1.0	6.1 ± 1.3	0.37
Liver histology					
Steatosis					
<1 %	139 (50.4)	67 (74.5)	53 (41.4)	19 (32.8)	
1–10 %	100 (36.2)	17 (18.9)	58 (45.3)	25 (43.1)	
11–33 %	26 (9.4)	3 (3.3)	15 (11.7)	8 (13.8)	
>33 %	11 (4.0)	3 (3.3)	2 (1.6)	6 (10.3)	
Activity grade[b]					
0	7 (2.5)	3 (3.3)	2 (1.5)	2 (3.5)	
1	120 (43.5)	42 (46.7)	60 (46.9)	18 (31.0)	
2	120 (43.5)	35 (38.9)	56 (43.8)	29 (50.0)	
3	29 (10.5)	10 (11.1)	10 (7.8)	9 (15.5)	
Fibrosis stage[b]					
0	10 (3.6)	3 (3.3)	4 (3.1)	3 (5.2)	
1	111 (40.2)	41 (45.6)	53 (41.4)	17 (29.3)	
2	83 (30.1)	26 (28.9)	40 (31.3)	17 (29.3)	
3	45 (16.3)	10 (11.1)	20 (15.6)	15 (25.9)	
4	27 (9.8)	10 (11.1)	11 (8.6)	6 (10.3)	

Values are mean ± standard deviation or numbers (%). Where no other unit is specified, values refer to numbers (%) of patients

ALT alanine aminotransferase, *AST* aspartate aminotransferase, *BMI* body mass index, *ND* not determined, *γ-GTP* γ-glutamyl transpeptidase

[a] Jonckheere–Terpstra test or Cochran–Armitage trend test

[b] According to reference [21]

analysis. Values of $p < 0.05$ were considered significant. Post hoc power analysis was performed using nQuery Advisor (Statistical Solutions, Boston, MA, USA).

Results

The characteristics of the 276 study subjects with chronic hepatitis C and the frequency distribution of the *PNPLA3* rs738409 C > G polymorphism are summarized in Table 1. The frequencies of the rs738409 CC, CG, and GG genotypes were 32.6, 46.4, and 21.0 %, respectively, and were in Hardy–Weinberg equilibrium. The rs738409 genotype was not significantly associated with clinical or biochemical factors, including age, sex, BMI, diabetes, HCV genotype, platelet count, and levels of serum AST, ALT, γ-GTP, albumin, and HCV-RNA.

We assessed the impact of the rs738409 genotype on histological liver damage in a cross-sectional manner. The prevalence of steatosis (defined as ≥1 %), severe

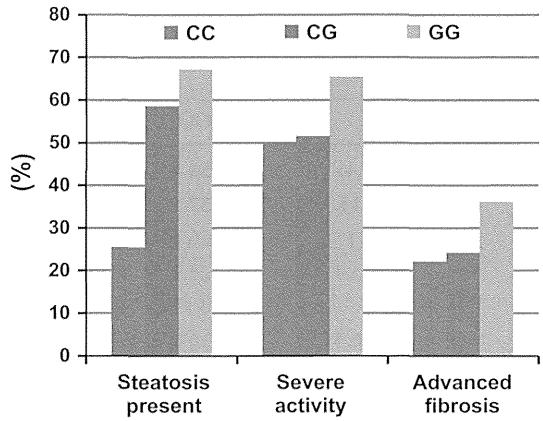

Fig. 1 The prevalence of steatosis (defined as ≥1 %), severe necroinflammatory activity (grade 2 or 3), and advanced fibrosis (stage 3 or 4) according to the *PNPLA3* rs738409 genotype

Table 2 Multivariable logistic regression analysis of the association of *PNPLA3* (rs738409 C>G), under a recessive inheritance model, with the presence of steatosis, severe necroinflammatory activity and advanced fibrosis

Variables	OR	95 % CI	*p*
Steatosis present (≥1 %)			
rs738409 (GG vs. CG + CC)	2.58	1.37–4.84	0.003
Age (years)	0.99	0.97–1.01	0.45
Sex (male vs. female)	1.19	0.70–2.02	0.51
BMI (kg/m^2)	1.19	1.10–1.30	<0.001
Diabetes (yes vs. no)	0.70	0.21–2.36	0.57
Severe necroinflammatory activity (grade 2 or 3)			
rs738409 (GG vs. CG + CC)	2.16	1.12–4.16	0.02
Age (years)	1.06	1.03–1.08	<0.001
Sex (male vs. female)	1.24	0.73–2.14	0.42
BMI (kg/m^2)	1.11	1.02–1.20	0.01
Diabetes (yes vs. no)	2.17	0.54–8.68	0.28
Advanced fibrosis (stage 3 or 4)			
rs738409 (GG vs. CG + CC)	2.10	1.07–4.11	0.03
Age (years)	1.07	1.04–1.10	<0.001
Sex (male vs. female)	1.31	0.72–2.40	0.38
BMI (kg/m^2)	1.14	1.04–1.24	0.006
Diabetes (yes vs. no)	1.77	0.52–6.05	0.37

BMI body mass index, *CI* confidence interval, *OR* odds ratio

necroinflammatory activity (grade 2 or 3), and advanced fibrosis (stage 3 or 4) according to the rs738409 genotype is shown in Fig. 1. Steatosis was present in 25.5, 58.6, and 67.2 %, severe necroinflammatory activity was found in 50.0, 51.6, and 65.5 %, and advanced fibrosis was found in 22.2, 24.2, and 36.2 % of patients with CC, CG, and GG genotypes, respectively.

To evaluate the effect of the rs738409 variant G allele, we used a recessive model of inheritance comparing G allele homozygotes (GG) with heterozygotes (CG) or C allele homozygotes (CC) (i.e., GG vs. CG + CC), according to previous reports [17, 18]. Multivariate analysis revealed that the GG genotype was independently associated with the presence of steatosis [odds ratio (OR) 2.58, 95 % confidence interval (CI) 1.37–4.84, $p = 0.003$], severe necroinflammatory activity (OR 2.16, 95 % CI 1.12–4.16, $p = 0.02$), and advanced fibrosis (OR 2.10, 95 % CI 1.07–4.11, $p = 0.03$), after adjustment for age, sex, BMI, and diabetes (Table 2). Besides the rs738409 GG genotype, a higher BMI was independently correlated with the presence of steatosis, severe necroinflammatory activity, and advanced fibrosis, and older age was independently associated with severe necroinflammatory activity and advanced fibrosis.

Discussion

In the present study, we showed that the *PNPLA3* rs738409 GG genotype was independently associated with the presence of steatosis, severe necroinflammatory activity, and advanced fibrosis in Japanese patients with CHC. Our results appear to be compatible with the following previous studies of European patients. The Swiss Hepatitis C Cohort Study [22] reported that the rs738409 G allele was associated with an increased risk of steatosis in Caucasian patients with HCV genotype non-3. The large Italian cross-sectional study [17] showed that the rs738409 GG genotype was associated with steatosis, fibrosis stage, cirrhosis, lower response to antiviral therapy, and hepatocellular carcinoma occurrence in CHC. In the cross-sectional and prospective study of Caucasian patients with CHC from Belgium, Germany, and France [18], the rs738409 GG genotype was associated with steatosis, fibrosis, and fibrosis progression.

However, to our knowledge, this is the first report to demonstrate the association of the *PNPLA3* rs738409 variant with advanced fibrosis in Japanese patients with CHC. Sato et al. [23] recently reported that the rs738409 GG genotype was associated with a higher prevalence of steatosis in Japanese patients with CHC, and Moritou et al. [24] showed that the rs738409 G allele tended to be associated with steatosis in such patients. In contrast, Nakamura et al. [25] reported that there was no correlation between the rs738409 genotype and steatosis and liver cirrhosis diagnosed by ultrasonography in Japanese patients with CHC. However, ultrasonography is a less accurate method for the diagnosis of steatosis and liver cirrhosis than the liver biopsy that was used in the present study.

Genotype frequency varies according to ethnicity. Importantly, our study, together with other studies of

Japanese patients with CHC [23–25], indicate that the frequency of the rs738409 GG genotype seems to be higher in Japanese patients (21.0–24.0 %) than in European patients (approximately 10 %) with CHC [17, 18]. If so, Japanese patients may be at higher risk for rapid progression of CHC than European patients.

Furthermore, several lines of evidence suggest the association of the rs738409 GG genotype with an increased risk of hepatocellular carcinoma in patients with CHC [17, 23, 26–28], although the association seems to be less pronounced in CHC than in alcoholic liver disease [26, 28].

Alcohol consumption is known to promote the development of steatosis and the progression of fibrosis in CHC. Müller et al. [29] found a distinct effect of the rs738409 genotype on steatosis and fibrosis in German patients with CHC according to the amount of alcohol intake; that is, while the rs738409 GG genotype was associated with steatosis only in abstainers (<30 g alcohol/day), it was associated with liver cirrhosis only in at-risk drinkers (>30 g alcohol/day). Valenti et al. [30] confirmed that the rs738409 GG genotype was associated with steatosis only in abstainers; however, they found that it was associated with cirrhosis in both abstainers and at-risk drinkers. Further studies are needed to examine the interaction between a moderate amount of alcohol intake and the rs738409 variant in CHC. In the present study, we excluded patients who consumed more than 20 g of alcohol per day to eliminate the confounding effect of alcohol on steatosis and fibrosis.

Although the rs738409 GG genotype was associated with severe necroinflammatory activity and advanced fibrosis, it was not related with a higher ALT level or a lower platelet count. The reason for this discrepancy is unknown. However, studies have shown that necroinflammatory activity grade is not well correlated with ALT levels in CHC [31, 32]. We may have failed to show the association of the GG genotype with a lower platelet count in part because the proportion of patients with advanced fibrosis (stage 3 or 4) was relatively low (26 %) and therefore the mean platelet count was not very low ($16.0 \times 10^4/\mu l$) in our patients.

Liver transplantation provides a unique opportunity to assess whether the effect of the rs738409 variant is localized in the liver or in other tissues, because transplantation creates a chimeric individual. A recent study of patients who underwent liver transplantation for hepatitis C in the United States showed that donor, but not recipient, rs738409 GG or CG genotype was associated with increased risk of fibrosis progression, retransplantation, or death after liver transplantation [33]. This finding indicated that the liver is indeed the site where the effect of the variant occurs. However, neither donor nor recipient rs738409 genotype was associated with hepatic steatosis during follow-up biopsies. These observations suggested that the rs738409 variant in the liver is responsible for fibrosis progression but not for steatosis. The rs738409 variant may influence the development of fibrosis and steatosis through different pathways.

PNPLA3 encodes a 481-amino acid protein that contains a highly conserved patatin-like domain at the N-terminal. PNPLA3 is a membrane-bound protein and is most highly expressed in the liver, followed by the skin and adipose tissue in humans [34, 35]. PNPLA3 expression is highly regulated by nutritional stimuli at both the transcriptional and posttranslational levels through the transcription factors SREBP-1c and liver X receptor [35–37]. Studies have found that levels of PNPLA3 were very low in the liver during fasting and were increased with carbohydrate feeding [35, 36].

Despite the strong clinical association of the *PNPLA3* rs738409 variant (I148 M) with liver diseases, the biochemical function of *PNPLA3* and the underlying mechanism by which the I148 M variant affects liver injury remain controversial. Some investigators have proposed that *PNPLA3* shows lipase activity and that the I148 M variant results in a loss of function [34, 38–40], while other authors have suggested that *PNPLA3* plays a role in lipid synthesis and that the I148 M variant exerts a gain-of-function effect [37, 41, 42]. Interestingly, Pirazzi et al. [40] reported that the wild-type *PNPLA3* has retinyl-palmitate lipase activity in human hepatic stellate cells, and that the lipase activity is markedly reduced in the I148 M variant. Because hepatic stellate cells are key players in fibrogenesis in chronic liver disease, *PNPLA3* may possibly be involved in the activation and transformation of hepatic stellate cells in response to hepatic injury and the development of liver fibrosis. Contrary to expectations, *PNPLA3*-deficient mice have not shown any obvious phenotype [43, 44]. However, it must be noted that there are differences in tissue-specific expression of *PNPLA3* between humans and mice [35].

Certain limitations should be considered in the interpretation of our findings. The cross-sectional study design hinders the ability to draw inferences regarding the causality of the rs738409 variant in histological liver damage. Although none of our patients had received any antiviral therapy before the liver biopsy, many of these patients had received ursodeoxycholic acid and herbal medicines. A past history of these treatments for CHC might have slightly influenced our results. A post hoc power analysis was performed using the actual sample size, based on the Chi-square test. Our study had sufficient power (more than 80 %) to detect a clinically meaningful effect size (odds ratio $\geq$2.4).

The *PNPLA3* rs738409 variant (I148 M) has now been associated with the progression of chronic liver diseases

with different etiologies, including NAFLD, alcoholic liver disease, and CHC. Moreover, the association appears to be common in different populations. Elucidation of the physiological functions of *PNPLA3* and the pathological effects of the I148 M variant will reveal the common underlying mechanisms involved in chronic liver diseases and may hopefully lead to identification of therapeutic targets for these diseases.

Acknowledgments This work was supported by a grant from the Ministry of Health, Labour and Welfare of Japan (H20-hepatitis-008 to Takeshi Okanoue, H24-hepatitis-general-006 to Takeshi Okanoue).

Conflict of interest The authors declare that they have no conflict of interest.

References

1. Poynard T, McHutchison J, Manns M, et al. Biochemical surrogate markers of liver fibrosis and activity in a randomized trial of peginterferon alfa-2b and ribavirin. Hepatology. 2003;38:481–92.
2. Leandro G, Mangia A, Hui J, et al. Relationship between steatosis, inflammation, and fibrosis in chronic hepatitis C: a meta-analysis of individual patient data. Gastroenterology. 2006;130:1636–42.
3. Negro F. Mechanisms and significance of liver steatosis in hepatitis C virus infection. World J Gastroenterol. 2006;12:6756–65.
4. Rubbia-Brandt L, Quadri R, Abid K, et al. Hepatocyte steatosis is a cytopathic effect of hepatitis C virus genotype 3. J Hepatol. 2000;33:106–15.
5. Yasui K, Harano Y, Mitsuyoshi H, et al. Steatosis and hepatic expression of genes regulating lipid metabolism in Japanese patients infected with hepatitis C virus. J Gastroenterol. 2010;45:95–104.
6. Wright M, Goldin R, Fabre A, et al. Measurement and determinants of the natural history of liver fibrosis in hepatitis C virus infection: a cross-sectional and longitudinal study. Gut. 2003;52:574–9.
7. Missiha SB, Ostrowski M, Heathcote EJ. Disease progression in chronic hepatitis C: modifiable and nonmodifiable factors. Gastroenterology. 2008;134:1699–714.
8. Romeo S, Kozlitina J, Xing C, et al. Genetic variation in PNPLA3 confers susceptibility to nonalcoholic fatty liver disease. Nat Genet. 2008;40:1461–5.
9. Valenti L, Al-Serri A, Daly AK, et al. Homozygosity for the patatin-like phospholipase-3/adiponutrin I148 M polymorphism influences liver fibrosis in patients with nonalcoholic fatty liver disease. Hepatology. 2010;51:1209–17.
10. Rotman Y, Koh C, Zmuda JM, et al. The association of genetic variability in patatin-like phospholipase domain-containing protein 3 (PNPLA3) with histological severity of nonalcoholic fatty liver disease. Hepatology. 2010;52:894–903.
11. Sookoian S, Pirola CJ. Meta-analysis of the influence of I148 M variant of patatin-like phospholipase domain containing 3 gene (PNPLA3) on the susceptibility and histological severity of nonalcoholic fatty liver disease. Hepatology. 2011;53:1883–94.
12. Tian C, Stokowski RP, Kershenobich D, et al. Variant in PNPLA3 is associated with alcoholic liver disease. Nat Genet. 2010;42:21–3.
13. Stickel F, Buch S, Lau K, et al. Genetic variation in the PNPLA3 gene is associated with alcoholic liver injury in Caucasians. Hepatology. 2011;53:86–95.
14. Trépo E, Gustot T, Degré D, et al. Common polymorphism in the PNPLA3/adiponutrin gene confers higher risk of cirrhosis and liver damage in alcoholic liver disease. J Hepatol. 2011;55:906–12.
15. Matteoni CA, Younossi ZM, Gramlich T, et al. Nonalcoholic fatty liver disease: a spectrum of clinical and pathological severity. Gastroenterology. 1999;116:1413–9.
16. Kawaguchi T, Sumida Y, Umemura A, et al. Genetic polymorphisms of the human PNPLA3 gene are strongly associated with severity of non-alcoholic fatty liver disease in Japanese. PLoS One. 2012;7:e38322.
17. Valenti L, Rumi M, Galmozzi E, et al. Patatin-like phospholipase domain-containing 3 I148 M polymorphism, steatosis, and liver damage in chronic hepatitis C. Hepatology. 2011;53:791–9.
18. Trépo E, Pradat P, Potthoff A, et al. Impact of patatin-like phospholipase-3 (rs738409 C > G) polymorphism on fibrosis progression and steatosis in chronic hepatitis C. Hepatology. 2011;54:60–9.
19. Committee of the Japan Diabetes Society on the Diagnostic Criteria of Diabetes Mellitus, Seino Y, Nanjo K, et al. Report of the committee on the classification and diagnostic criteria of diabetes mellitus. J Diabetes Investig. 2010;1:212–28.
20. Simmonds P, Alberti A, Alter HJ, et al. A proposed system for the nomenclature of hepatitis C viral genotypes. Hepatology. 1994;19:1321–4.
21. Poynard T, Bedossa P, Opolon P. Natural history of liver fibrosis progression in patients with chronic hepatitis C. The OBSVIRC, METAVIR, CLINIVIR, and DOSVIRC groups. Lancet. 1997;349:825–32.
22. Cai T, Dufour JF, Muellhaupt B, et al. Viral genotype-specific role of PNPLA3, PPARG, MTTP, and IL28B in hepatitis C virus-associated steatosis. J Hepatol. 2011;55:529–35.
23. Sato M, Kato N, Tateishi R, et al. Impact of PNPLA3 polymorphisms on the development of hepatocellular carcinoma in patients with chronic hepatitis C virus infection. Hepatol Res. 2014;44:E137–44.
24. Moritou Y, Ikeda F, Iwasaki Y, et al. Impact of comorbid hepatic steatosis on treatment of chronic hepatitis C in Japanese patients and the relationship with genetic polymorphism of IL28B, PNPLA3 and LDL receptor. Acta Med Okayama. 2014;68:17–22.
25. Nakamura M, Kanda T, Nakamoto S, et al. No correlation between PNPLA3 rs738409 genotype and fatty liver and hepatic cirrhosis in Japanese patients with HCV. PLoS One. 2013;8:e81312.
26. Nischalke HD, Berger C, Luda C, et al. The PNPLA3 rs738409 148 M/M genotype is a risk factor for liver cancer in alcoholic cirrhosis but shows no or weak association in hepatitis C cirrhosis. PLoS One. 2011;6:e27087.
27. Falleti E, Fabris C, Cmet S, et al. PNPLA3 rs738409C/G polymorphism in cirrhosis: relationship with the aetiology of liver disease and hepatocellular carcinoma occurrence. Liver Int. 2011;31:1137–43.
28. Trépo E, Nahon P, Bontempi G, et al. Association between the PNPLA3 (rs738409 C > G) variant and hepatocellular carcinoma: Evidence from a meta-analysis of individual participant data. Hepatology. 2014;59:2170–7.
29. Müller T, Buch S, Berg T, et al. Distinct, alcohol-modulated effects of PNPLA3 genotype on progression of chronic hepatitis C. J Hepatol. 2011;55:732–3.
30. Valenti L, Colombo M, Fargion S. Modulation of the effect of PNPLA3 I148 M mutation on steatosis and liver damage by alcohol intake in patients with chronic hepatitis C. J Hepatol. 2011;55:1470–1.
31. Haber MM, West AB, Haber AD, et al. Relationship of aminotransferases to liver histological status in chronic hepatitis C. Am J Gastroenterol. 1995;90:1250–7.

32. Okanoue T, Makiyama A, Nakayama M, et al. A follow-up study to determine the value of liver biopsy and need for antiviral therapy for hepatitis C virus carriers with persistently normal serum aminotransferase. J Hepatol. 2005;43:599–605.
33. Dunn W, O'Neil M, Zhao J, et al. Donor PNPLA3 rs738409 genotype affects fibrosis progression in liver transplantation for hepatitis C. Hepatology. 2014;59:453–60.
34. He S, McPhaul C, Li JZ, et al. A sequence variation (I148 M) in PNPLA3 associated with nonalcoholic fatty liver disease disrupts triglyceride hydrolysis. J Biol Chem. 2010;285:6706–15.
35. Huang Y, He S, Li JZ, et al. A feed-forward loop amplifies nutritional regulation of PNPLA3. Proc Natl Acad Sci USA. 2010;107:7892–7.
36. Lake AC, Sun Y, Li JL, et al. Expression, regulation, and triglyceride hydrolase activity of Adiponutrin family members. J Lipid Res. 2005;46:2477–87.
37. Li JZ, Huang Y, Karaman R, et al. Chronic overexpression of PNPLA3 I148 M in mouse liver causes hepatic steatosis. J Clin Invest. 2012;122:4130–44.
38. Pirazzi C, Adiels M, Burza MA, et al. Patatin-like phospholipase domain-containing 3 (PNPLA3) I148 M (rs738409) affects hepatic VLDL secretion in humans and in vitro. J Hepatol. 2012;57:1276–82.
39. Pingitore P, Pirazzi C, Mancina RM, et al. Recombinant PNPLA3 protein shows triglyceride hydrolase activity and its I148 M mutation results in loss of function. Biochim Biophys Acta. 2014;1841:574–80.
40. Pirazzi C, Valenti L, Motta BM, et al. PNPLA3 has retinyl-palmitate lipase activity in human hepatic stellate cells. Hum Mol Genet. 2014;23:4077–85.
41. Kumari M, Schoiswohl G, Chitraju C, et al. Adiponutrin functions as a nutritionally regulated lysophosphatidic acid acyltransferase. Cell Metab. 2012;15:691–702.
42. Kumashiro N, Yoshimura T, Cantley JL, et al. Role of patatin-like phospholipase domain-containing 3 on lipid-induced hepatic steatosis and insulin resistance in rats. Hepatology. 2013;57:1763–72.
43. Chen W, Chang B, Li L, Chan L. Patatin-like phospholipase domain-containing 3/adiponutrin deficiency in mice is not associated with fatty liver disease. Hepatology. 2010;52:1134–42.
44. Basantani MK, Sitnick MT, Cai L, et al. Pnpla3/Adiponutrin deficiency in mice does not contribute to fatty liver disease or metabolic syndrome. J Lipid Res. 2011;52:318–29.

Liver INTERNATIONAL

Liver International ISSN 1478-3223

NAFLD & NASH

Blockade of interleukin 6 signalling ameliorates systemic insulin resistance through upregulation of glucose uptake in skeletal muscle and improves hepatic steatosis in high-fat diet fed mice

Kanji Yamaguchi[1], Takeshi Nishimura[1], Hiroshi Ishiba[1], Yuya Seko[1], Akira Okajima[1], Hideki Fujii[1], Nozomi Tochiki[1], Atsushi Umemura[1], Michihisa Moriguchi[1], Yoshio Sumida[1], Hironori Mitsuyoshi[1], Kohichiroh Yasui[1], Masahito Minami[1], Takeshi Okanoue[2] and Yoshito Itoh[1]

1 Molecular Gastroenterology and Hepatology, Graduate School of Medical Science, Kyoto Prefectural University of Medicine, Kyoto, Japan
2 Department of Gastroenterology & Hepatology, Saiseikai Suita Hospital, Osaka, Japan

Keywords
HFD – IL-6 – insulin resistance – leptin – NAFLD – STAT3

Abbreviations
ACOX, acyl-CoA oxidase 1; ALT, alanine aminotransferase; AMPK, adenosine monophosphate-activated protein kinase; AST, aspartate aminotransferase; CPT1, carnitine palmitoyltransferase 1; FAS, fatty acid synthase; FFA, free fatty acids; GLUT, glucose transporter type; GTT, glucose tolerance test; GUS, glucuronidase; HFD, high-fat diet; IL-6, Interleukin-6; IR, insulin resistance; ITT, insulin tolerance test; LDL-R, low density lipoprotein-receptor; MCD, methionine choline deficiency; NAFLD, nonalcoholic fatty liver disease; NASH, nonalcoholic steatohepatitis; PPAR, peroxisome proliferator-activated receptor; RA, rheumatoid arthritis; SAA, serum amyloid A; SOCS, suppressor of cytokine signalling; SREBP, sterol regulatory element-binding protein; STAT, signal transducer and activator of transcription; T2DM, type 2 diabetes mellitus; T-CHO, total cholesterol; TNF-α, tumour necrosis factor-alpha.

Correspondence
Kanji Yamaguchi, MD, PhD
Molecular Gastroenterology and Hepatology,
Graduate School of Medical Science, Kyoto Prefectural University of Medicine,
465 Kajii-cho, Kawaramachi-Hirokoji,
Kamigyou-ku,
Kyoto 602-8566, Japan
Tel: +81 75 251 5519
Fax: +81 75 251 0710
e-mail: ykanji@koto.kpu-m.ac.jp

Received 1 March 2014
Accepted 23 July 2014

DOI:10.1111/liv.12645
Liver Int. 2015; 35: 550–561

Abstract

Background & Aims: Mice fed high-fat diet (HFD) demonstrate obesity-related systemic insulin resistance (IR). Aim of this study is to clarify the role of interleukin (IL)-6 in IR *in vivo* focusing on skeletal muscle, adipose tissue and liver. *Methods:* Plasma markers of IR and hepatic IL-6 signalling were examined in eight-week HFD feeding C57/BL6 mice. Furthermore, IR-related molecules in skeletal muscles, adipose tissues and livers were investigated following a single injection of anti- IL-6 receptor neutralizing antibody (MR16-1) in two-week HFD feeding mice. To investigate the role of IL-6 in hepatic steatosis by prolonged HFD, hepatic triglyceride accumulation was assessed in eight-week HFD feeding mice with continuous MR16-1 treatment. *Results:* High-fat diet for both 2 and 8 weeks elevated plasma IL-6, insulin and leptin, which were decreased by MR16-1 treatment. A single injection of MR16-1 ameliorated IR as assessed by glucose and insulin tolerance test, which may be attributable to upregulation of glucose transporter type 4 via phosphorylation of AMP-activated protein kinase as well as upregulation of peroxisome proliferator-activated receptor alpha in livers and, particularly, in skeletal muscles. MR16-1 also decreased mRNA expression of leptin and tumour necrosis factor-alpha and increased that of adiponectin in adipose tissue. High-fat diet for 8 weeks, not 2 weeks, induced hepatic steatosis and increased hepatic triglyceride content, all of which were ameliorated by MR16-1 treatment. *Conclusions:* Blockade of excessive IL-6 stimulus ameliorated HFD-induced IR in a skeletal muscle and modulated the production of adipokines from an early stage of NAFLD, leading to prevention of liver steatosis for a long term.

Nonalcoholic fatty liver disease (NAFLD) is one of the most common liver diseases worldwide (1). The incidence of NAFLD is growing with the increasing prevalence of metabolic syndrome. It is estimated that one-third of subjects with NAFLD suffer from nonalcoholic steatohepatitis (NASH) and that 10-15% develop cirrhosis (2). A key role in the development of NAFLD has been attributed to obesity and insulin resistance (IR), which are associated with a state of chronic inflammation (3–6). This association was inferred in part because circulating pro-inflammatory cytokines and adipokines were reported to be elevated and they were considered independent risk factors for type 2 diabetes mellitus (T2DM) (7–10). IL-6 produced by adipocytes, monocytes/macrophages and endothelial cells is classified as a pro-inflammatory cytokine, having been shown to modify insulin sensitivity, and is a predictor of the development of T2DM (6, 7, 10). IL-6 is an inhibitor of insulin action in isolated hepatocytes, hepatoma cell lines, 3T3L-1 adipocytes, and livers of experimental mice and leads to IR *in vivo* when chronically administered to mice at levels similar to those found in obese individuals (11–15). However, recent reports have demonstrated a beneficial effect of IL-6 as a myokine (16, 17). Muscle-derived IL-6 activates AMP-activated protein kinase (AMPK) in both skeletal muscle and adipose tissue and enhances glucose uptake and fatty acid oxidation in skeletal muscle (18–20). Furthermore, short-term administration of IL-6 in an *in vivo* mouse model elevated IL-6 with unimpaired insulin action but enhanced glucose tolerance (21, 22). In summary, chronic elevations in IL-6 may impair insulin signalling in hepatocytes and adipocytes, but acute IL-6 administration could enhance insulin sensitivity in muscle. A recent report stated that HbA1c decreased in diabetic patients with rheumatoid arthritis (RA) who were treated with a humanized anti-IL-6 receptor neutralizing antibody, tocilizumab (23). This finding suggested that inhibition of IL-6 signalling in patients with RA and diabetes resulted in a favourable outcome. Clinically, in patients with NAFLD, IL-6/signal transducer and activator of transcription 3 (STAT3) signalling may be excessively upregulated and may induce systemic IR through induction of suppressor of cytokine signalling 3 (SOCS3) in various organs (7–10, 24). Recent studies of human NASH have shown that hepatic IL-6 expression correlates positively with plasma IL-6 levels and degree of hepatic inflammation, stage of fibrosis and systemic IR (9). These findings suggest a possible role of IL-6 as a pro-inflammatory cytokine in the development of human and mouse NASH.

From a different point of view, IL-6 is believed to aggravate liver inflammation, whereas IL-6 is well known to be a hepatoprotective cytokine (25–29). We have recently reported in methionine choline deficient (MCD) diet-fed mice that blockade of interleukin-6 signalling by neutralizing antibody against the IL-6 receptor (MR16-1), which is a specific antagonist of the mouse IL-6 receptor, reduced liver injury in wild type lean mice but exacerbated liver injury by promoting hepatocyte apoptosis in db/db mice (30–32). These differing observations between wild type and db/db mice in a NASH model indicate a paradoxical role for IL-6 in the development of chronic inflammation and the promotion of hepatocyte proliferation. We speculated that, although an excess of IL-6 may act as a mediator of inflammation in human and mouse NASH, in some experimental models with severely suppressed IL-6-STAT3 signalling, such as STAT3−/−, IL-6 Receptor−/−, or Glycoprotein130−/− mice, IL-6 may play a hepatoprotective role and exert an anti-obesity effect against various types of liver injury including steatohepatitis (25, 26, 29). In our earlier studies, we used a MCD diet-induced NASH model that did not exhibit systemic IR and could not reveal the effect of IL-6 on IR in the development of NAFLD (31, 32). Accordingly, in this study, we focused on the role of IL-6 in the aetiology of IR and NAFLD and investigated the effect of inhibition of IL-6 signalling on HFD-induced IR in mouse livers, muscles and adipose tissues.

Material and methods

Animals and treatments

A mouse model of diet-induced obesity was studied. Eight-week-old male C57/BL6 mice were purchased from Japan Jackson Laboratories, maintained in a temperature- and light-controlled facility, and permitted consumption of water *ad libitum*. Five mice were fed a control chow diet and 10 were fed a high-fat diet (HFD; D12492; Research Diet Inc., Tokyo, Japan) for 8 weeks. Half of the HFD-fed mice were treated with 15 mg/kg rat antimouse IL-6 receptor antibody (MR16-1; Cyugai Pharmaceutical Co. Ltd., Tokyo, Japan) intraperitoneally (i.p.) twice weekly, whereas the remainder and the chow-fed mice were injected with control rat IgG (Equitech-Bio, Inc., Kerrville, TX, USA) (30–32). Another 24 mice were fed HFD for 2 weeks and then injected i.p. with either MR16-1 or control IgG (12 mice for each). At 48 h following the single injection, half of the mice fasted for 7 h were treated with or without insulin (1.0 U/kg body weight) through i.p. injection. Fifteen minutes later, livers, skeletal muscles (gastrocnemius), epididymal fats, and blood were isolated. The remaining mice of each group were used for glucose tolerance test (GTT) and insulin tolerance test (ITT) respectively. All animal experiments fulfilled the requirements for humane animal care in Kyoto Prefectural University of Medicine.

Glucose and insulin tolerance tests

Intraperitoneal glucose (2 g/kg body weight) and insulin (0.75 U/kg body weight) tolerance tests were

performed after 16- and 7-h fasts, respectively, and blood glucose was measured at the time indicated. For insulin release during glucose tolerance testing, the plasma component of blood collected at the 0-, 30-min, 1-h and 2-h time points was measured with an insulin enzyme immunoassay system, the Morinaga ultrasensitive mouse insulin assay kit (Morinaga Institute of Biological Science, Inc., Kanagawa, Japan).

Immunoblot assay

Proteins isolated from whole livers and gastrocnemius were separated by SDS-PAGE and transferred to PVDF membranes. Membranes were probed with anti-STAT3, antiphospho-STAT3 at Tyr705, anti-Akt, antiphospho-Akt at Thr308 and Ser473, anti-AMPK, antiphospho-AMPK at Thr172, anti-IRS-1(Cell Signaling Technology Inc., Beverly, MA, USA), antiphospho-IRS-1 at Tyr896 (Sigma-Aldrich, Tokyo, Japan), anti-PPARα (LifeSpan Biosciences, Inc., Seattle, WA, USA), anti-GLUT4, or anti-actin (Santa-Cruz Biotechnology, Inc., Santa-Cruz, CA, USA) antibody, followed by horseradish peroxidase (HRP)-conjugated antimouse or rabbit IgG (GE Healthcare, Tokyo, Japan). Antigens were visualized by ECL (GE Healthcare). Immunoblots of IRS-1 were scanned, and band intensities were quantified by Image J (NIH) densitometry analysis.

Two-step real-time RT-PCR

Total RNA was extracted from whole livers with RNeasy kits (Qiagen, Valencia, CA, USA), reversetranscribed using random primer and Superscript RNase H-reverse transcriptase (Invitrogen, Carlsbad, CA, USA), and analysed by real-time PCR as described (33). Specificity was confirmed for all primer pairs by sequencing of the PCR products. The mouse primers used were SOCS3 sense primer, 5-GGGTGGCAAAGAAAAGGAG-3; SOCS3 antisense primer, 5-GTTGAGCGTCAAGACCC AGT-3; TNF-α sense primer, 5-AAGCCTGTAGCCCA CGTCGTA-3; TNF-α antisense primer, 5-AGGTACAA CCCATCGGCTGG-3; FAS sense primer, 5-CATGAC CTCGTGATGAACGTGT-3; FAS antisense primer, 5-C GGGTGAGGACGTTTACAAAG-3; CPT-1 sense primer, 5-TCCATGCATACCAAAGTGGA-3; CPT-1 antisense primer, 5-TGGTAGGAGAGCAGCACCTT-3; ACOX1 sense primer, 5-GCCCAACTGTGACTTCCATC-3; ACOX1 antisense primer, 5-GCCAGGACTATCGCAT GATT-3; SREBP-1c sense primer, 5-GCAGTCTGCTT TGGAACCTC-3; SREBP-1c antisense primer, 5-CCAC AAAGAAACGGTGACCT-3; LDL-R sense primer, 5-CC ACTTCCGCTGCAAATCAT-3;LDL-R antisense primer, 5-TCATGGGAGCCGTCAACAC-3; GLUT4 sense primer, 5-9AAAAGTGCCTGAAACCAGAG-3; GLUT4 antisense primer, 5-TCACCTCCTGCTCTAAAAGG-3; Adiponectin sense primer, 5-AAGGACAAGGCCGTTC TCT-3; Adiponectin antisense primer, 5-TATGGGTAG TTGCAGTCAGTTGG-3; Leptin sense primer, 5-CCAA AACCCTCATCAAGACC-3; Leptin antisense primer, 5-GTCCAACTGTTGAAGAATGTCCC-3; GUS sense primer, 5-GCAGTTGTGTGGGTGAATGG-3; and GUS antisense primer, 5-GGGTCAGTGTGTTGTTGATG G-3. Target gene levels were presented as a ratio of levels intreated vs. corresponding control groups. Fold changes were determined using point and interval estimates.

Haematoxylin and eosin (H&E) staining

Serial sections of livers were stained with H & E using standard techniques.

Tissue and plasma biochemical measurements

Plasma aspartate aminotransferase (AST), alanine aminotransferase (ALT), free fatty acids (FFA), total cholesterol (T-CHO) and triglyceride levels were measured as follows (33). Plasma IL-6, plasma serum amyloid A (SAA), plasma leptin, plasma adiponectin concentrations and tissue triglyceride were measured using an IL-6 Mouse ELISA Kit (R&D Systems, Minneapolis, MN, USA), SAA Mouse ELISA Kit (Streassgen, Victoria, Canada), Mouse Leptin ELISA Kit (Morinaga, Yokohama, Japan), Mouse Adiponectin/Acrp30 Quantikine ELISA Kit (R&D Systems) and Triglyceride Detection Kit (Sigma-Aldrich) according to the manufacturers' instructions.

Statistical analysis

Results were expressed as mean ± SEM. Significance was established using two-way repeated ANOVA (Fig. 2c) or Student's *t*-test, and analysis of variance where appropriate. Differences were considered significant at $P < 0.05$.

Results

HFD-induced hyperlipidaemia and systemic insulin resistance with the elevation of plasma IL-6 levels

High-fat diet for 8 weeks greatly increased plasma triglycerides, T-CHO, free fatty acid, glucose, ALT value, fasting insulin and leptin levels, whereas plasma adiponectin levels were similar between chow- and HFD-fed mouse groups (Table 1). Plasma IL-6 levels were consistently higher in HFD- than those in chow-fed mice (Fig. 1a). Because IL-6 is the major inducer of hepatic acute phase proteins, plasma SAA levels were also measured. As expected, these levels were significantly elevated in HFD-fed mice (Fig. 1a). To evaluate hepatic IL-6/GP130 signalling, we assessed mRNA levels of IL-6, IL-6 receptor (R) and SOCS3, and protein levels of STAT3. HFD increased hepatic IL-6 mRNA but not IL-6 R (Fig. 1b). Consistently, hepatic STAT3 was strongly activated in HFD-fed mice (Fig. 1c), and hepatic mRNA levels of SOCS3, which is induced by phosphorylated STAT3, were marginally increased (Fig. 1d). Taken

Table 1. Plasma biochemical parameters at 8 weeks

Diet	Chow diet	HFD	
Treatment	Control IgG	Control IgG	MR16-1
Triglyceride (mg/dl)	44.0 ± 4.1	58.4 ± 2.5**	56.0 ± 3.0
Total cholesterol (mg/dl)	132.8 ± 3.0	228.8 ± 7.1**	186.4 ± 5.9††
Free fatty acid (mg/dl)	697.2 ± 70.2	949.2 ± 108.2*	886.4 ± 53.7
ALT (U/L)	22.4 ± 0.7	39.6 ± 2.0**	38.8 ± 2.4
Glucose (mg/dl)	204.7 ± 21.8	258.4 ± 13.4**	234.5 ± 7.6 (P = 0.09)
Insulin (ng/ml)	0.59 ± 0.03	1.30 ± 0.10**	0.71 ± 0.12†
Leptin (ng/ml)	4.2 ± 0.9	32.1 ± 9.1**	11.3 ± 2.8††
Adiponectin (ng/ml)	4.7 ± 0.2	4.9 ± 0.1	4.8 ± 0.2
IL-6 (pg/ml)	Not detected	2.95 ± 1.99	32.9 ± 5.7††

*P < 0.05; **P < 0.01. Chow diet vs. HFD.
†P < 0.05; ††P < 0.01. HFD + control IgG vs. HFD + MR16-1.

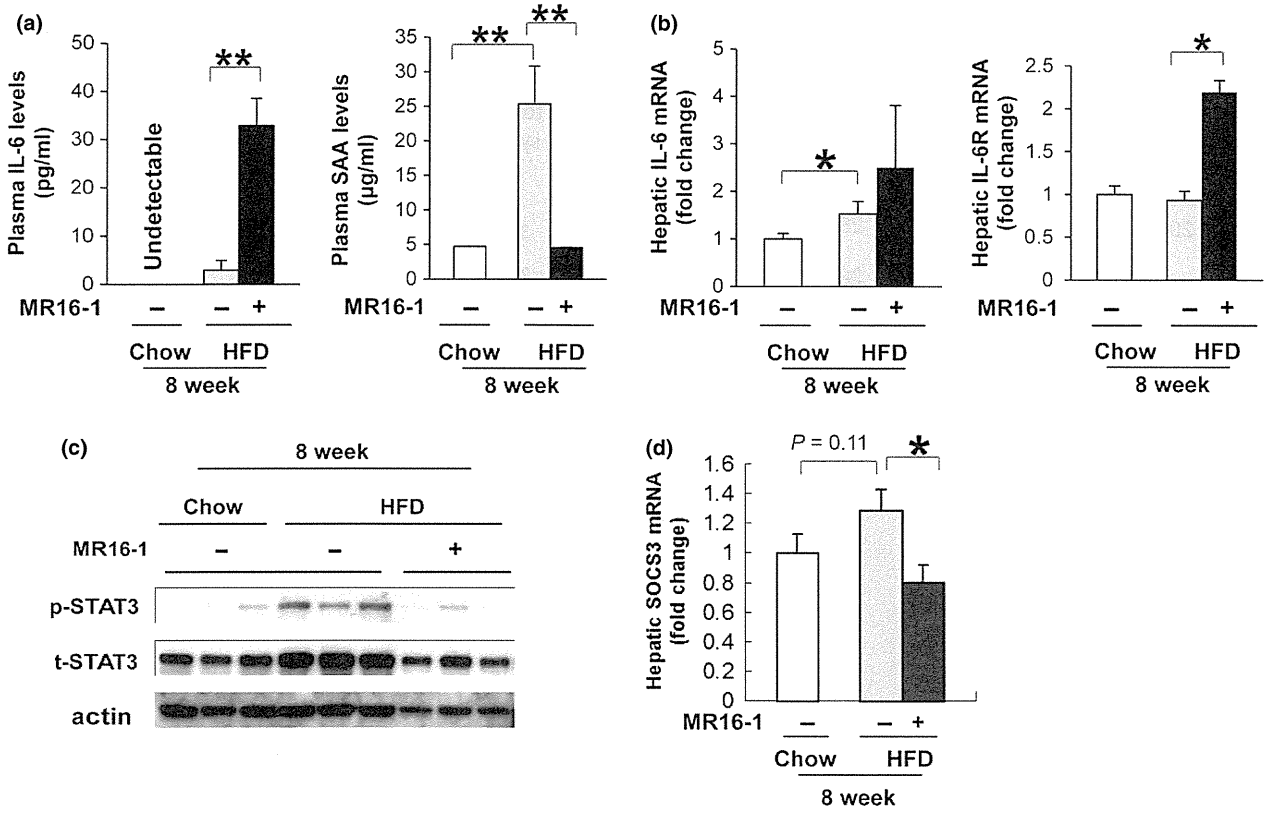

Fig. 1. The effect of HFD for eight week on hepatic IL-6 signalling (a) Plasma IL-6 and SAA levels were measured. Mean ± SE data from each group (n = 5/group) are plotted at 8 weeks (**P < 0.01). (b) Hepatic mRNA levels of IL-6 and IL-6R were determined by quantitative real-time PCR analysis of total liver RNA obtained after 8 weeks. Results were normalized to glucuronidase (GUS) expression in each sample and then expressed as fold change relative to gene expression in chow-fed control mice. Mean ± SE data from each group (n = 5/group) (*P < 0.05). (c) Phosphorylated (p)-STAT3 and total (t)-STAT3 levels were evaluated by immunoblot analysis of livers from three mice/group after 8 weeks. To control for loading, the blot was stripped and re-probed for actin, a housekeeping gene. (d) Hepatic mRNA levels of SOCS3 were determined by quantitative real-time PCR analysis of total liver RNA obtained after 8 weeks. Results were normalized to glucuronidase (GUS) expression in each sample and then expressed as fold change relative to gene expression in chow-fed control mice. Mean ± SE data from each group (n = 5/group) (*P < 0.05).

together, we concluded that HFD for 8 weeks induced IR with the elevation of plasma levels of IL-6 and the activation of hepatic IL-6 signalling including upregulation of SOCS3 expression. The latter expression has been reported to have an inhibitory effect on insulin signalling.

HFD for 2 weeks also induced IR with the elevation of plasma IL-6 levels and this response was ameliorated by single injection of IL-6 receptor neutralizing antibody (MR16-1)

Obesity and liver steatosis themselves are major cause of systemic insulin resistance. Therefore, to assess the effect of IL-6 on IR prior to developing obesity and hepatic lipid accumulation, we used 15 mg/kg IL-6 receptor neutralizing antibody (MR16-1) to block the IL-6/GP130 pathway and assayed IR-related markers and gene expression in various organs following a single intraperitoneal injection of MR16-1 into mice fed with HFD for 2 weeks. HFD for even 2 weeks elevated plasma IL-6, SAA (Fig. 2a), fasting glucose and insulin levels (Fig. 2b) and led to systemic insulin resistance (Fig. 2c). A single injection of MR16-1 decreased plasma SAA (Fig. 2a), glucose and insulin levels (Fig. 2b). When neutralizing IL-6 receptor by MR16-1 increased plasma IL-6 and decreased SAA levels (Fig. 2a), fasting glucose and insulin levels were significantly decreased (Fig. 2b). Furthermore, GTT and ITT revealed that MR16-1 treatment clearly ameliorated systemic IR (Fig. 2c).

Treatment with MR16-1 for 2 weeks suppressed mRNA levels of SOCS3 expression in livers, muscles and adipose tissues

IL-6, IL-6R and SOCS3 expression was assessed by real-time PCR in livers, adipose tissues and skeletal muscles. IL-6 and SOCS3 expression was high in skeletal muscles, whereas livers expressed predominately IL-6R mRNA (Fig. 3a, b). MR16-1 treatment slightly increased hepatic IL-6 mRNA levels and significantly suppressed SOCS3 mRNA, which has been reported to be a key molecule in IL-6 induced IR through inhibition of insulin, leptin and IL-6 signalling, in various organs (Fig. 3a, b).

The effect of neutralizing the IL-6 receptor in a liver

To determine why a single injection of MR16-1 ameliorated systemic IR, we investigated hepatic insulin and

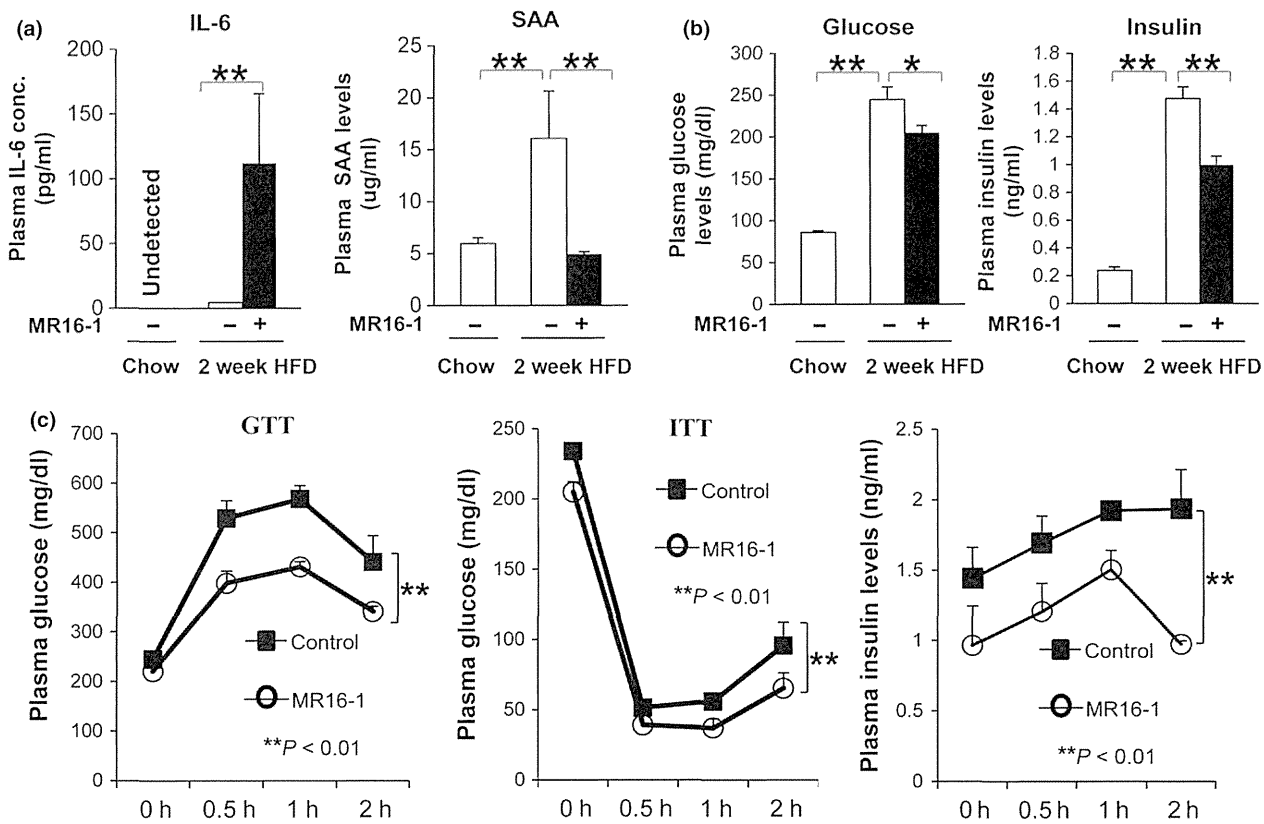

Fig. 2. The effect of a single injection of MR16-1 on markers of systemic insulin resistance in HFD-fed mice for 2 weeks (a) Plasma IL-6 and SAA levels were measured at 48 h following the single injection of MR16-1 treatment. Mean ± SE data from each chow-fed control and HFD diet-fed group (n = 5/group) are plotted (**P < 0.01). (b) Plasma glucose and insulin levels were also determined in each group (n = 5/group). Data are presented as Mean ± SE (*P < 0.05, **P < 0.01). (c) Intraperitoneal glucose and insulin tolerance test at 48 h following the single injection of MR16-1 to mice fed with HFD for 2 weeks (n = 3/group) were graphed. Plasma insulin levels were also determined in each group (n = 3/group) at the 0-, 30-min, 1-h and 2-h time points. Data are presented as Mean ± SE. Significance was established using two-way repeated ANOVA (**P < 0.01).

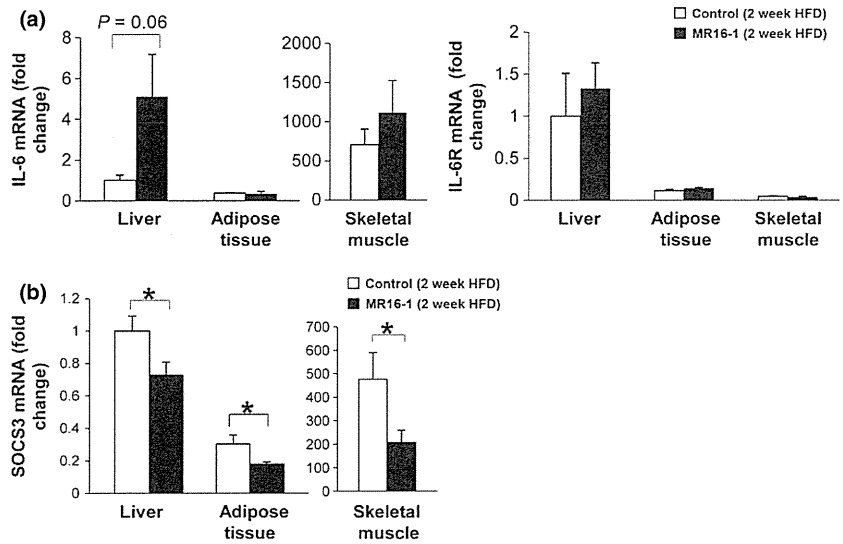

Fig. 3. The effect of a single injection of MR16-1 on SOCS3 expression in livers, adipose tissues and skeletal muscles of mice fed with HFD for 2 weeks (a) mRNA levels of IL-6 and IL-6R in livers, skeletal muscles and adipose tissues were determined by quantitative real-time PCR analysis. Results were normalized to GUS expression and then expressed as fold changes relative to gene expression in control IgG-treated mice. Mean ± SE data from each group (n = 3/group). (B) mRNA levels of SOCS3 were also determined by quantitative real-time PCR analysis. Mean ± SE data from each group (n = 3/group) (*P < 0.05).

IL-6-related signalling. MR16-1 treatment decreased both baseline and insulin-stimulated phosphorylation levels of STAT3 (Fig. 4a). Insulin-stimulated phosphorylation of IRS-1 at Tyr896 was increased by MR16-1 (Fig. 4b). Consistently, baseline phosphorylation of Akt at Thr308 and Ser473, which are required for the activation of insulin signalling, were increased by MR16-1 treatment (Fig. 4b), whereas insulin-stimulated phosphorylation of Akt was similar between the two groups of mice. Interestingly, baseline phosphorylation of AMPK and insulin-stimulated protein levels of peroxisome proliferator-activated receptor alpha (PPARα) were significantly increased by MR16-1 treatment (Fig. 4c) but protein levels of glucose transporter type 2 (GLUT2) were not increased (data not shown). Furthermore, we examined lipid-related gene expressions, such as fatty acid synthase (FAS), sterol regulatory element-binding protein (SREBP)-1c, GLUT2, carnitine palmitoyltransferase 1 (CPT1), acyl-CoA oxidase 1 (ACOX1) and low density lipoprotein-receptor (LDL-R), by real-time PCR and found that hepatic mRNA of CPT1 and LDL-R were greatly increased by MR16-1 and that SREBP-1c was slightly decreased (Fig. 4d), suggesting that MR16-1 treatment enhanced hepatic lipid oxidation through upregulation of AMPK and PPARα expression.

The effect of neutralizing the IL-6 receptor in a skeletal muscle

To evaluate other mechanisms of improvement of systemic IR by MR16-1, we analysed IL-6-, insulin- and lipid oxidation-related gene expression in skeletal muscles. MR16-1 treatment significantly decreased phosphorylation of STAT3 levels and mRNA levels of SOCS3 in skeletal muscles (Fig. 3, Fig. 5a). While MR16-1 treatment had no effect of phosphorylation of IRS-1 at Tyr896, insulin-stimulated phosphorylation of Akt at Thr308 and baseline phosphorylation of Akt at Ser473 was increased (Fig. 5b). Furthermore and interestingly, both baseline and insulin-stimulated phosphorylation levels of AMPK were greatly increased in MR16-1 treated mice (Fig. 5c). Protein levels of GLUT4 and PPARα were also increased by MR16-1 with and without insulin injection (Fig. 5c). Because mRNA levels of GLUT4 were significantly increased and those of CPT1 and ACOX1 marginally increased by MR16-1 treatment, we concluded that MR16-1 treatment ameliorated IR clearly because of promotion of glucose uptake and lipid oxidation through the upregulation of AMPK and PPARα in skeletal muscles (Fig. 5d).

The effect of neutralizing the IL-6 receptor on adipokines in an adipose tissue

We assessed the effect of MR16-1 treatment on adipokine expression in adipose tissue. TNF-α mRNA levels in adipose tissue were greatly suppressed by MR16-1 treatment (Fig. 6a) and, surprisingly, mRNA levels of leptin were significantly decreased and adiponectin were increased by MR16-1 in mice fed HFD for 2 weeks (Fig. 6b). Plasma adiponectin levels were similar between both groups (Fig. 6c), whereas plasma leptin levels were significantly lower in MR16-1-treated than control mice (Fig. 6c). These observations suggested that MR16-1 treatment not only suppressed

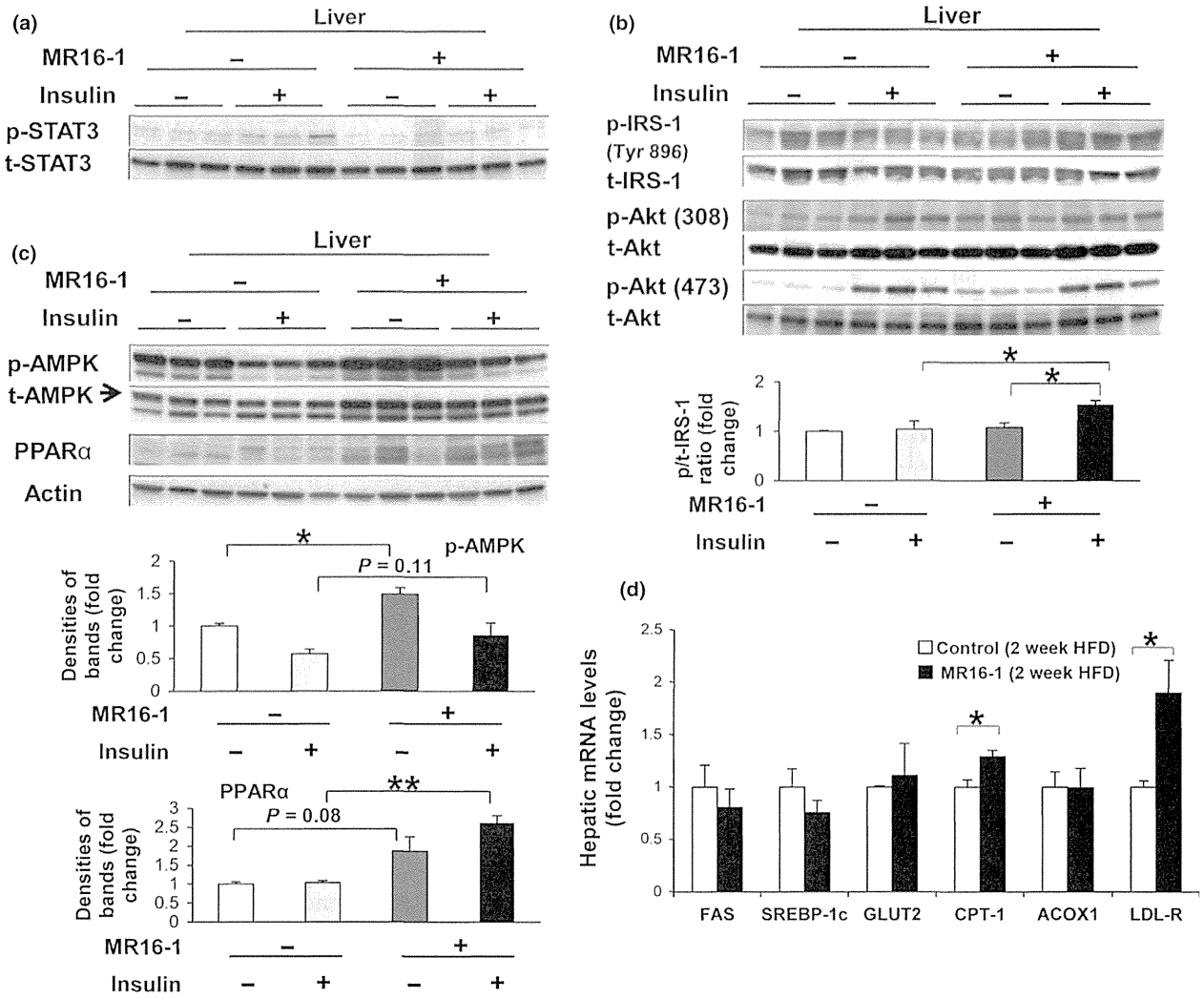

Fig. 4. The effect of a single injection of MR16-1 in livers (a) Baseline and insulin-stimulated phosphorylated (p)-STAT3 and total (t)-STAT3 levels were evaluated by immunoblot analysis of livers from three mice/group at 48 h following the single injection of MR16-1. To control for loading, the blot was stripped and re-probed for actin, a housekeeping gene. (b) Baseline and insulin-stimulated p-IRS-1, total t-IRS-1, p-Akt at Tyr308 and Ser473 and t-Akt levels were evaluated by immunoblot analysis of livers from three mice/group. P-IRS-1/t-IRS-1 ratio in each group were also expressed as fold change in controls (*$P < 0.05$). (c) Baseline and insulin-stimulated p-AMPK, t-AMPK and PPARα levels were evaluated by immunoblot analysis of livers from three mice/group. P-AMPK and PPARα in each group were also expressed as fold change in controls (*$P < 0.05$, **$P < 0.01$). (d) Hepatic mRNA levels of FAS, SREBP-1c, GLUT2, CPT-1, ACOX1 and LDL-R were determined by quantitative real-time PCR analysis. Results were normalized to GUS expression and then expressed as fold changes relative to gene expression in control IgG-treated mice. Mean ± SE data from each group ($n = 3$/group) (*$P < 0.05$).

HFD-induced fat inflammation and leptin overexpression but also might restore adiponectin expression in adipose tissue.

Neutralizing IL-6 receptor by MR16-1 treatment for 8 weeks ameliorated HFD-induced obesity and hepatic steatosis

IL-6 could promote systemic IR in livers and skeletal muscles, and modulates expressions of adipokines in adipose tissues even in an earlier phase of NAFLD prior to obvious obesity and hepatic steatosis. Mice fed HFD for 8 weeks exhibited obesity (Fig. 7a), due mainly to hypertrophic adipose tissue (Fig. 7b) and hepatic steatosis (Fig. 7c) with increased liver weights and liver triglyceride content (Fig. 7b, d) despite a reduction in liver/BW ratio (Fig. 7b). To examine the effect of long-term replacement of MR16-1 on HFD-induced NAFLD model, treatment with MR16-1 for 8 weeks twice a week was performed in HFD-fed mice. Similar to our previous study (31, 32), plasma IL-6 levels were elevated by MR16-1 treatment, whereas plasma SAA levels were significantly reduced (Fig. 1a). Hepatic phosphorylation of STAT3 and mRNA levels of SOCS3 were also

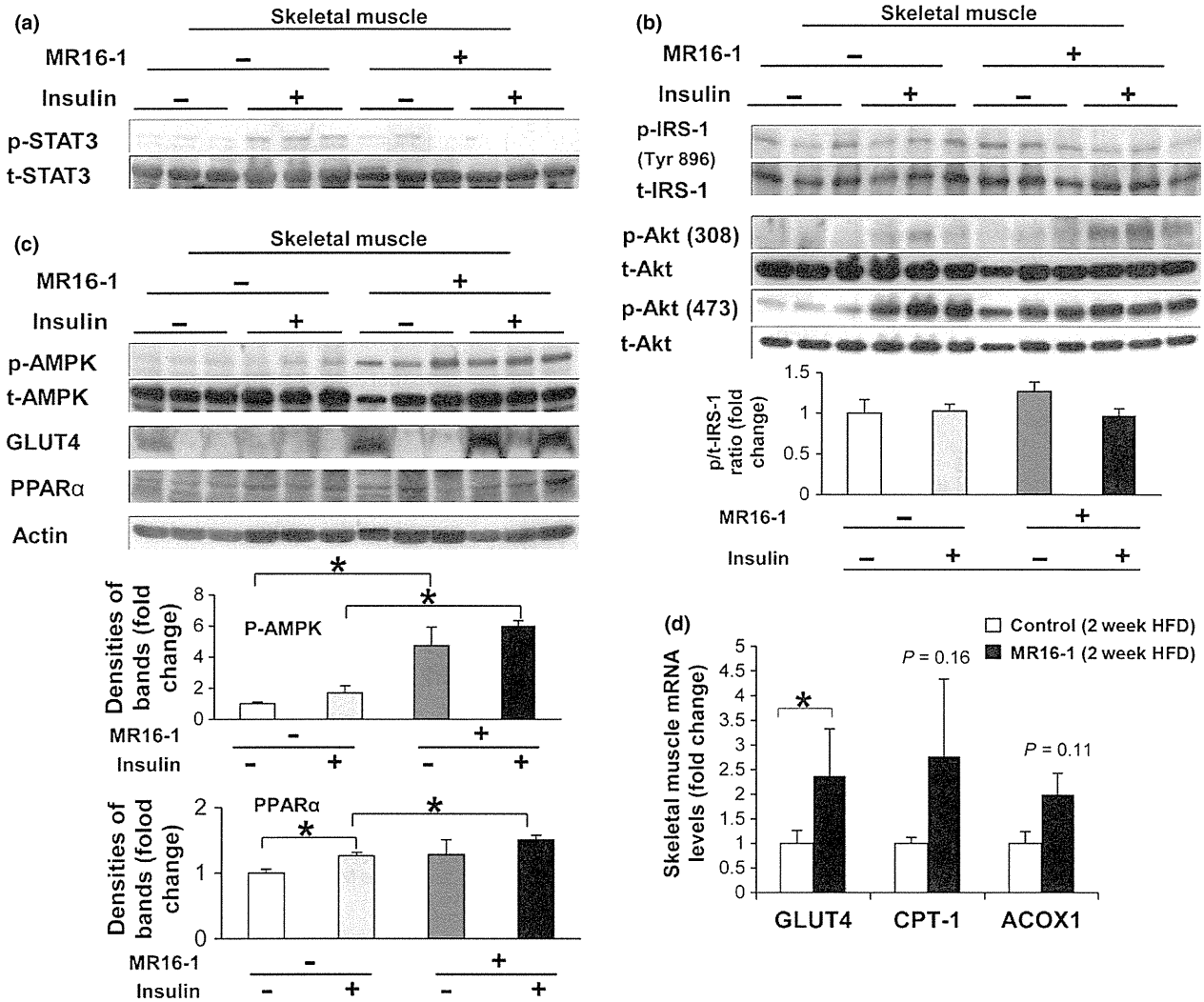

Fig. 5. The effect of a single injection of MR16-1 in skeletal muscles (a) Baseline and insulin-stimulated p-STAT3 and total t-STAT3 levels were evaluated by immunoblot analysis of skeletal muscles from three mice/group at 48 h following the single injection of MR16-1. (b) Baseline and insulin-stimulated p-IRS-1, total t-IRS-1, p-Akt at Tyr308 and Ser473 and t-Akt levels were evaluated by immunoblot analysis of skeletal muscles from threre mice/group. P-IRS-1/t-IRS-1 ratio in each group were also expressed as fold change in controls (*$P < 0.05$). (c) Baseline and insulin-stimulated p-AMPK, t-AMPK, GLUT4 and PPARα levels were evaluated by immunoblot analysis of skeletal muscles from three mice/group. To control for loading, the blot was stripped and re-probed for actin, a housekeeping gene. P-AMPK and PPARα in each group were also expressed as fold change in controls (*$P < 0.05$). (d) Skeletal muscle mRNA levels of hepatic GLUT4, CPT-1 and ACOX1were determined by quantitative real-time PCR analysis. Results were normalized to GUS expression and then expressed as fold changes relative to gene expression in control IgGtreated mice. Mean ± SE data from each group (n = 3/group) (*$P < 0.05$).

significantly decreased (Fig. 1b, c), suggesting that MR16-1 successfully blocked IL-6 signalling during 8 weeks. We found that MR16-1 treatment reduced BW (Fig. 7a), liver/BW ratio, epididymal/BW ratio (Fig. 7b), and hepatic steatosis, as shown by H&E staining of liver sections (Fig. 7c). To confirm the reduction in hepatic steatosis by MR16-1, we assessed liver triglyceride content and found that MR16-1 treatment significantly reduced it (Fig. 7d). To determine why MR16-1 treatment ameliorated liver steatosis, in this study we focused on the improvement of systemic IR by MR16-1. However, although we assessed hepatic insulin signalling by Western blotting for phosphorylated IRS and Akt in MR16-1-treated mice fed HFD for 8 weeks as well as those in HFD-fed mice for 2 weeks, MR16-1 treatment had little effect on hepatic insulin signalling (data not shown), in part because baseline plasma levels of glucose, insulin and leptin, BW and liver steatosis had already been ameliorated by repeated MR16-1 treatment during the eight-week HFD feeding.

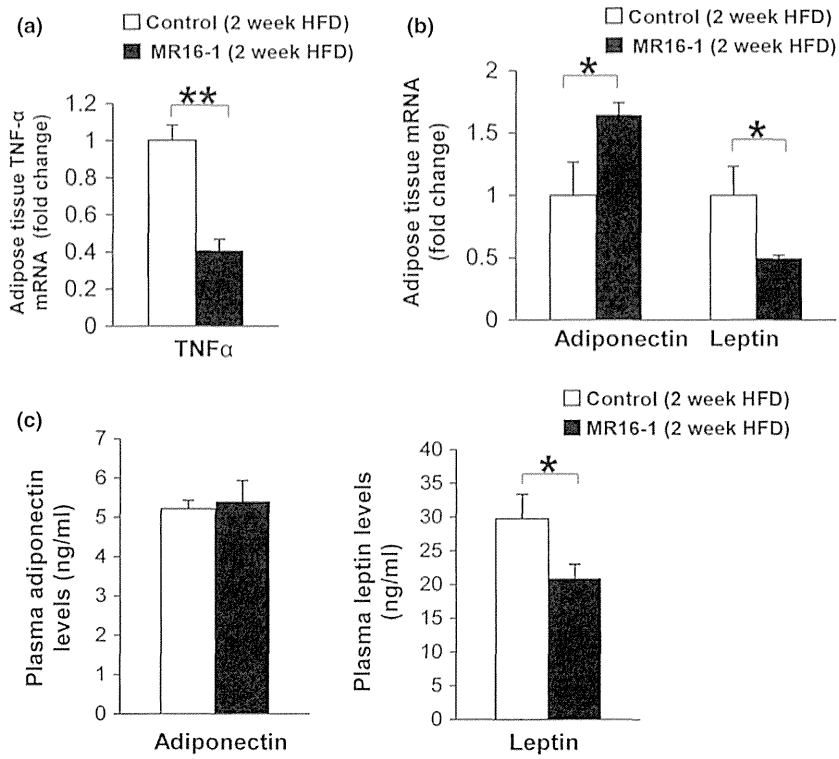

Fig. 6. The effect of a single injection of MR16-1 on adipokines expression (a) mRNA levels of TNF-α in adipose tissues were determined by quantitative real-time PCR analysis. Results were normalized to GUS expression and then expressed as fold changes relative to gene expression in control IgG-treated mice. Mean ± SE data from each group (n = 3/group) (**P < 0.01). (b) mRNA levels of adiponectin and leptin in adipose tissues were determined by quantitative real-time PCR analysis. Results were normalized to GUS expression and then expressed as fold changes relative to gene expression in control IgGtreated mice. Mean ± SE data from each group (n = 3/group) (*P < 0.05). (c) Plasma adiponectin and leptin levels were determined in each group (n = 3/group). Data are presented as Mean ± SE (*P < 0.05).

Discussion

In this study, we showed that continuous IL-6 stimulation was closely associated with IR, mainly in skeletal muscles, from an early stage of NAFLD and induced intrahepatic lipid accumulation gradually for a long term. These observations indicate that IL-6-induced IR in muscles is a major cause of obesity and hepatic lipid accumulations. As seen in human NAFLD, despite absence of fibrosis or obvious inflammation, mice fed with a HFD for 8 weeks induced obesity, systemic IR and hepatic steatosis with the elevation of plasma IL-6 levels and upregulation of IL-6/GP130-related genes in livers, and all of these responses were ameliorated by IL-6 receptor neutralizing antibody (Figs 1,7). To confirm this beneficial effect of IL-6 blocking, we focused on the association between systemic IR and comparative longer IL-6 exposure, and assessed insulin signalling in livers, skeletal muscles and adipose tissues separately in only two-week HFD-induced mouse NAFLD. Despite absence of even obesity or hepatic steatosis, HFD for 2 weeks induced systemic IR with the elevation of plasma IL-6 levels and this response was also ameliorated by MR16-1 treatment (Fig. 2a–c). Blockade of IL-6 signalling by MR16-1 treatment clearly promoted glucose uptake and lipid oxidation mediated by AMPK and PPARα in skeletal muscles (Fig. 5c, d), and repaired the imbalance of adipokines in adipose tissues (Fig. 6b, c). These findings indicated that IL-6 may play a key role in the induction of systemic IR rather than in evoking inflammation/fibrosis in an early stage of NAFLD. Collectively, the improvement of systemic IR by inhibiting chronic IL-6 stimulation may be a potential therapeutic strategy for avoiding the development of NAFLD.

IL-6 has been reported to have both favourable and unfavourable actions on metabolic responses in a liver, skeletal muscle and adipose tissue (7, 9–23, 29, 34, 35). However, elevated plasma IL-6 observed in IR status of HFD-fed mice did not work as a 'myokine'. This study showed that inhibition of IL-6 signalling by MR16-1 treatment dramatically induced phosphorylation of AMPK and increased GLUT4 and PPARα expression in skeletal muscle despite little effect on phosphorylation of IRS-1 at Thr896 (Fig. 5b, c), contributing to increased glucose uptake and lipid oxidation independently of insulin stimulation and resulting in the improvement of plasma glucose levels. In the liver, MR16-1 treatment increased insulin-stimulated

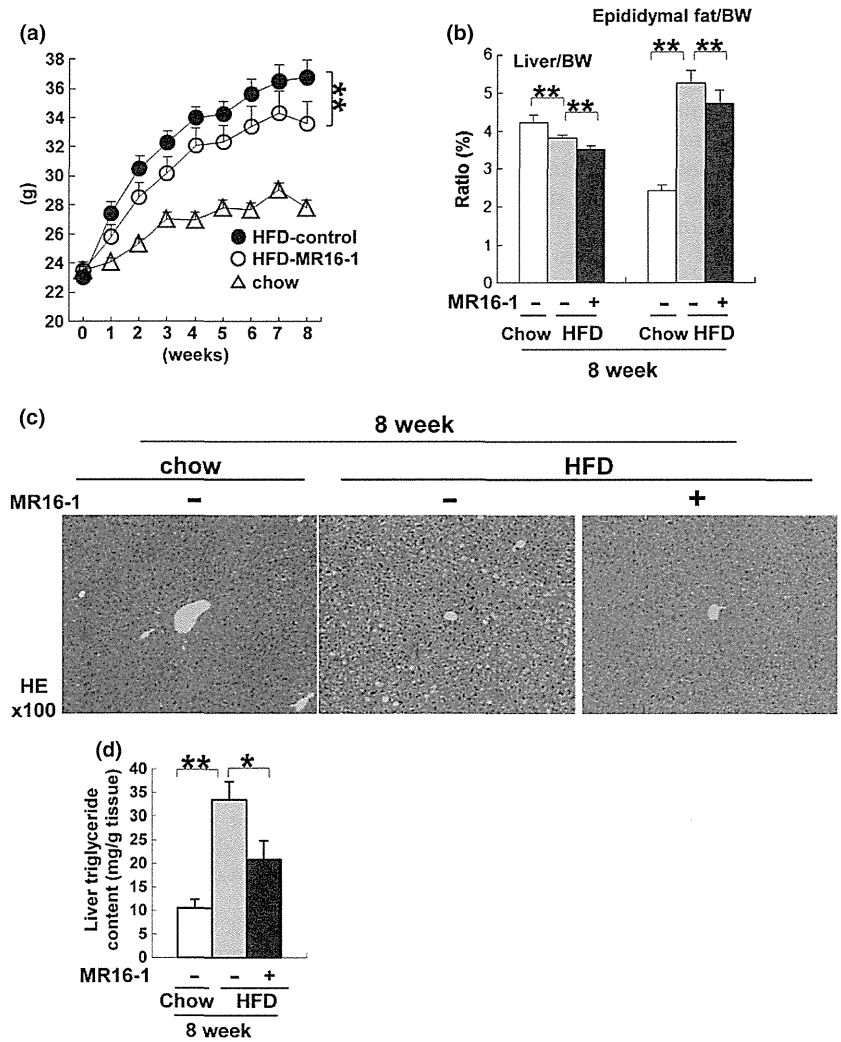

Fig. 7. The effect of MR16-1 treatment for eight weeks on HFD-induced mouse NAFLD (a) Body weight changes during 8 week-MR16–1 treatment are plotted. Mean ± SE data from each group are plotted at each week (**$P < 0.01$). (b) Liver/body weight (BW) and epididymal fat/BW ratio (%) were assessed at the end of treatment. Mean ± SE data from each group are plotted at 8 weeks (**$P < 0.01$). (c) Haematoxylin and eosin staining of liver sections from representative mice from each treatment group. (d) Liver triglycerides also were measured. Results are expressed per gram tissue. Mean ± SE data from each group are plotted at 8 weeks (*$P < 0.05$, **$P < 0.01$).

phosphorylation of IRS-1 at Thr896 (Fig. 4b), tended to increase baseline phosphorylation of AMPK and clearly increased insulin-stimulated PPARα (Fig. 4c) despite no elevation of GLUT2 expression (Fig. 4d), suggesting that inhibition of hepatic IL-6 signalling may tend to ameliorate IR and enhance AMPK- and PPARα-related lipid oxidation. At a glance, these observations contradicted the role of muscle-derived IL-6 as a 'myokine'. However, we speculate that chronic IL-6 stimulation in a chronic inflammatory state exerts an effect on glucose and lipid metabolism different from that in acute IL-6 exposure as a myokine, given that SOCS3 elevated by IL-6 and other cytokines in a chronic inflammatory state plays a key role in an unfavourable response to glucose and lipid metabolism in skeletal muscles and livers. In fact, SOCS3 expression in livers and skeletal muscles of HFD-fed mice was decreased by a single injection of MR16-1 (Fig. 3). SOCS3 is well known to suppress insulin signalling through directly inhibiting phosphorylation of insulin receptor substrate, leptin-related JAK-STAT signalling, and AMPK signalling, so that a reduction in excessive and continuous SOCS3 expression can restore the activities of those pathways (34–36). In this study, blocking effect of IL-6 signalling by MR16-1 may look like more obvious in skeletal muscles than that in livers and, interestingly, expression levels of IL-6 and SOCS3 were much higher in skeletal muscle than those in other tissues (Fig. 3).

MR16-1 treatment decreased plasma insulin and leptin levels (Table 1, Fig. 2b and Fig. 6c). Decreased

plasma leptin levels, which usually parallel to decreased plasma insulin levels in various situations, may attribute to reduced leptin secretion from adipose tissues by MR16-1 treatment (Fig. 6b, c) (37). Furthermore, consistent with previous reports showing that adiponectin gene expression and secretion were also inhibited by IL-6, a single injection of MR16-1 increased adiponectin expression (Fig. 6b) but not, unfortunately, plasma levels of adiponectin (Fig. 6c), suggesting that chronic IL-6 stimulation directly dysregulates adipokine production in adipose tissue (38).

We suspected that improvement of plasma leptin levels through a decrease in SOCS3 expression by MR16-1 played an important role in this experimental model. This hypothesis is supported by the finding in our preliminary study of mouse chow and HFD models in db/db mice, which lack ObRb and exhibited an enhanced obesity and liver steatosis after MR16-1 treatment despite decreased plasma levels of insulin (data not shown). Obesity-related hyperleptinemia and leptin signalling could enhance IL-6-related SOCS3 expression and decrease ObR-dependent AMPK phosphorylation (39, 40). The reduction in SOCS3 expression by MR16-1 improved plasma leptin levels and restored ObR-dependent AMPK activities in skeletal muscles and livers, leading to upregulation of glucose uptake, lipid oxidation and improvement of systemic insulin resistance.

We conclude that chronic elevation of IL-6 is closely associated with insulin resistance and enhance obesity and liver steatosis in HFD-fed mice. Inhibition of IL-6 signalling by MR16-1 suppressed excess SOCS3 expression in livers, skeletal muscles, and adipose tissues and ameliorated insulin resistance. Although these findings are results of synergic interaction of the beneficial effects of inhibiting IL-6 signalling in livers, skeletal muscles and adipose tissues, greatly enhanced GULT4 expression in skeletal muscles may be a key point. This finding is consistent with the recent evidence that IR in skeletal muscles promotes hepatic steatosis in the elderly patients, which is restored by excise (41, 42). Here, MR16-1 quickly ameliorated IR in skeletal muscles and prevented hepatic steatosis. We propose that further studies using MR16-1 in murine NASH models with systemic IR, such as a high-cholesterol diet-fed model (43), will reveal the significance of IL-6 signalling in NASH.

Acknowledgements

Financial support: This study was supported by Grant-in-Aid for Scientific Research from the Japan Society for the Program of Science (Kanji Yamaguchi and Yoshito Itoh).

Conflict of interest: Yoshito Itoh has received a research grant from Chugai Pharmaceutical Co., Ltd. The rest of the authors do not have any disclosures to report.

References

1. Ludwig J, Viggiano TR, McGill DB, Ott BJ. Nonalcoholic steatohepatitis: mayo clinic experience with a hitherto unnamed disease. *Mayo Clinic Proc* 1980; **55**: 434–8.
2. Chalasani N, Younossi Z, Lavine JE, *et al.* The diagnosis and management of non-alcoholic fatty liver disease: practice guideline by the American gastroenterological association, American association for the study of liver diseases, and American college of gastroenterology. *Gastroenterology* 2012; **142**: 1592–609.
3. Kahn SE, Hull RL, Utzschneider KM Mechanisms linking obesity to insulin resistance and type 2 diabetes. *Nature.* 2006;**444**:840–6. Review.
4. Tilg H, Moschen AR. Inflammatory mechanisms in the regulation of insulin resistance. *Mol Med* 2008; **14**: 222–31.
5. Utzschneider KM, Kahn SE. Review: the role of insulin resistance in nonalcoholic fatty liver disease. *J Clin Endocrinol Metab* 2006; **91**: 4753–61.
6. Guilherme A, Virbasius JV, Puri V, Czech MP. Adipocyte dysfunctions linking obesity to insulin resistance and type 2 diabetes. *Nat Rev Mol Cell Biol* 2008; **9**: 367–77.Review.
7. Maachi M, Piéroni L, Bruckert E, *et al.* Systemic low-grade inflammation is related to both circulating and adipose tissue TNFalpha, leptin and IL-6 levels in obese women. *Int J Obes Relat Metab Disord* 2004; **28**: 993–7.
8. Jarrar MH, Baranova A, Collantes R, *et al.* Adipokines and cytokines in non-alcoholic fatty liver disease. *Aliment Pharmacol Ther* 2008; **27**: 412–21.
9. Wieckowska A, Papouchado BG, Li Z, *et al.* Increased hepatic and circulating interleukin-6 levels in human nonalcoholic steatohepatitis. *Am J Gastroenterol* 2008; **103**: 1372–9.
10. Pradhan AD, Manson JE, Rifai N, Buring JE, Ridker PM. C-reactive protein, interleukin 6, and risk of developing type 2 diabetes mellitus. *JAMA* 2001; **286**: 327–34.
11. Rotter V, Nagaev I, Smith U. Interleukin-6 (IL-6) induces insulin resistance in 3T3-L1 adipocytes and is, like IL-8 and tumor necrosis factor-alpha, overexpressed in human fat cells from insulin-resistant subjects. *J Biol Chem* 2003; **278**: 45777–84.
12. Kim HJ, Higashimori T, Park SY, *et al.* Differential effects of interleukin-6 and -10 on skeletal muscle and liver insulin action *in vivo*. *Diabetes* 2004; **53**: 1060–7.
13. Senn JJ, Klover PJ, Nowak IA, Mooney RA. Interleukin-6 induces cellular insulin resistance in hepatocytes. *Diabetes* 2002; **51**: 3391–9.
14. Klover PJ, Zimmers TA, Koniaris LG, Mooney RA. Chronic exposure to interleukin-6 causes hepatic insulin resistance in mice. *Diabetes* 2003; **52**: 2784–9.
15. Klover PJ, Clementi AH, Mooney RA. Interleukin-6 depletion selectively improves hepatic insulin action in obesity. *Endocrinology* 2005; **146**: 3417–27.
16. Pedersen BK, Febbraio MA. Muscle as an endocrine organ: focus on muscle-derived interleukin-6. *Physiol Rev* 2008; **88**: 1379–406. Review.
17. Pedersen BK, Fischer CP. Beneficial health effects of exercise–the role of IL-6 as a myokine. *Trends Pharmacol Sci* 2007; **28**: 152–6.
18. Al-Khalili L, Bouzakri K, Glund S, *et al.* Signaling specificity of interleukin-6 action on glucose and lipid metabolism in skeletal muscle. *Mol Endocrinol* 2006; **20**: 3364–75.